


OPEN ACCESS

Review—A Comparative Evaluation of Redox Mediators for Li-O₂ Batteries: A Critical Review

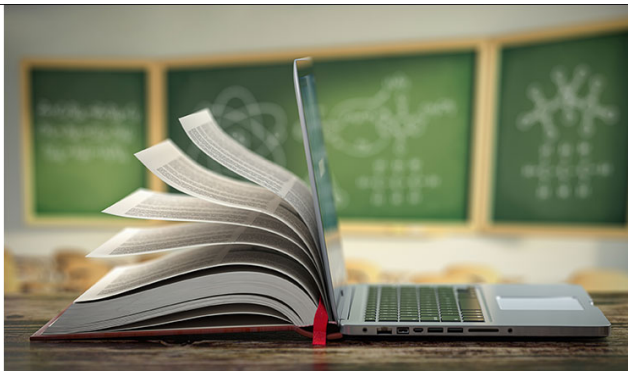
To cite this article: Won-Jin Kwak *et al* 2018 *J. Electrochem. Soc.* **165** A2274

View the [article online](#) for updates and enhancements.

 The Electrochemical Society
Advancing solid state & electrochemical science & technology
2021 Virtual Education

Fundamentals of Electrochemistry:
Basic Theory and Kinetic Methods
Instructed by: **Dr. James Noël**
Sun, Sept 19 & Mon, Sept 20 at 12h–15h ET

Register early and save!





Review—A Comparative Evaluation of Redox Mediators for Li-O₂ Batteries: A Critical Review

Won-Jin Kwak,¹ Hun Kim,¹ Hun-Gi Jung,² Doron Aurbach,^{3,*} and Yang-Kook Sun^{1,**,z}

¹Department of Energy Engineering, Hanyang University, Seoul 04763, Korea

²Center for Energy Convergence Research, Green City Technology Institute, Korea Institute of Science and Technology, Seoul 02792, Korea

³Department of Chemistry and BINA (BIU Institute of Nano-technology and Advanced Materials), Bar-Ilan University, Ramat-Gan 5290002, Israel

For resolving the low-energy efficiency issue of Li-O₂ batteries, many kinds of redox mediators (RMs) have been adapted. However, studies looking into the problems of RMs in these systems are insufficient. We compare herein effects and problems of RMs in Li-O₂ batteries by applying unique methodology, based on two types of cells, comparison between argon and oxygen atmospheres and combining electrochemistry in conjunction with spectroscopy. Using systematic electrochemical measurements, representative RMs in Li-O₂ battery prototypes were thoroughly explored with respect to oxygen presence, voltage ranges and scan rates. By this comparative, multi-parameters study we reached valuable insights. We identified possible routes for RMs degradation in Li-O₂ batteries related to the cathode side, using bi-compartments cells with solid electrolyte that blocks the crossover between the cathode and the Li metal sides. Based on comparative electrochemical and spectroscopic analyses, we confirmed that degradation of the RMs activity was caused by intrinsic decomposition of the RMs in the electrolyte solution at the cathode part, even before further reactions with reduced oxygen species. This work provides a realistic view of the role of important RMs in Li-oxygen cells and suggests guidelines for effective screening and selecting suitable RMs, mandatory components in Li-O₂ batteries.

© The Author(s) 2018. Published by ECS. This is an open access article distributed under the terms of the Creative Commons Attribution 4.0 License (CC BY, <http://creativecommons.org/licenses/by/4.0/>), which permits unrestricted reuse of the work in any medium, provided the original work is properly cited. [DOI: 10.1149/2.0901810jes]



Manuscript submitted May 25, 2018; revised manuscript received July 8, 2018. Published July 24, 2018.

As the demand for batteries used in portable electrical devices, such as cell phones, cameras, and laptops, in electric vehicles, and even in large energy storage systems is soaring, the requirements and performance demands are also rapidly increasing. However, the development rate of battery performance in terms of capacity, efficiency, energy density, life span, and stability is very slow and has not been able to follow the accelerated development of other industries in recent years. Moreover, the energy density of conventional Li-ion batteries, the best battery systems available today, is theoretically limited and is much lower than that of the energy supply systems based on fossil fuels (e.g., internal combustion engines). Therefore, the development of next-generation high-performance batteries is a key issue to satisfy the increasing demand for high energy density and surpass the limitations of the currently used Li-Ion batteries.¹⁻³ Among the options, lithium oxygen (Li-O₂) batteries, in which the active mass of the cathodes is oxygen from air, have very high theoretical energy density because the main cathode material does not contribute to the weight and volume of the battery. In fact, if Li-O₂ batteries become practically operational, they may be able to rival internal combustion engines in terms of energy density.¹⁻³ Such characteristic will enable worldwide use of electric vehicles, even for long distance driving. In Li-O₂ cells based on non-aqueous Li salt solutions, oxygen is reduced to lithium peroxide (Li₂O₂) as the main discharge product. In fact, the mechanism of oxygen reduction in non-aqueous solutions containing Li cations may be complicated, involves the formation of unstable moieties such as superoxide species, and is accompanied by undesirable (even detrimental) side reactions. Decomposition of Li₂O₂ back to molecular oxygen may need high over-voltages that endanger the stability of most relevant solvents and the carbonaceous materials that usually compose the cathodes. Therefore, in order to make effective Li-O₂ cells, the use of appropriate catalysts in the cells is crucially important.

In recent years, leading researchers in the field have reported on improvements in Li-O₂ battery models by using modified cathodes,^{4,5} more suitable electrolyte solutions,^{6,7} and protected Li anodes.^{8,9} However, several flaws need to be resolved in order to promote these

systems to practical, real life applications.¹⁰⁻¹² Among the issues, the formation of uncontrollable discharge products by side reactions is a major problem. The need of too high over-voltages for the anodic (charging) reaction, namely oxidation of the Li₂O₂ formed by oxygen reduction, is another key disadvantage.¹³ There are also surface passivation problems if the Li₂O₂ is deposited as a film on the cathode.^{14,15} Finally, the use of Li metal anodes in these systems involves the usual drawbacks associated with such a reactive metal in rechargeable batteries.¹⁶⁻¹⁸ Because of these problems, Li-O₂ batteries exhibit limited specific capacity (well below the theoretical value), capacity fading, low energy efficiency, and poor cyclability.^{14,19} Moreover, if the over-potential during charge is higher than 4.0 V vs. Li, the steady operation suffers from electrode and electrolyte solution decomposition by side oxidation reactions.^{20,21}

Various types of solid catalysts have been adopted to promote the reversible decomposition of Li₂O₂ at a low enough charge potential, in order to avoid oxidative side reactions and to increase energy efficiency and cyclability.²²⁻²⁸ However, the activity of many solid catalysts decreases during cycling of Li-O₂ batteries because direct contact between the solid catalysts and the main oxygen reduction product, Li₂O₂, is prevented by accumulation of side products. These are formed mostly by electrolyte solution degradation via parasitic reactions with the highly reactive superoxide and peroxide species in solution, promoted by the solid catalysts.^{29,30} Such side reactions can lead to disappearance of the electrolyte solution in the cells upon cycling, and a consequent cell termination.³¹⁻³³

The necessary catalysis in Li-O₂ cells can be much more effective if the solid catalysts deposited on the cathodes' surface can be replaced by redox mediators (RMs) in the solution phase. The red-ox potentials of the relevant RMs should be slightly higher than the potential required for Li₂O₂ oxidation. Hence, upon charging, the RM in solution is oxidized first via electron transfer from open sites on the cathode surface (not blocked by Li₂O₂ deposits); then, the oxidized RM moieties react with the LiO₂ deposits from the solution side, and hence, all the Li₂O₂ formed during discharge can be fully oxidized back to molecular oxygen, without any limitation of electron transfer from the solid cathode to the electronically insulating Li₂O₂ deposits.³⁴⁻⁴¹ The RMs for Li-O₂ cells can be selected according to their unique specific redox reaction potentials. In general, the use of

*Electrochemical Society Fellow.

**Electrochemical Society Member.

^zE-mail: yksun@hanyang.ac.kr; Doron.Aurbach@biu.ac.il

RMs in Li-O₂ cells exhibits more effective and reproducible results than the use of solid catalysts.

However, previous reports showed that the catalytic effects of RMs in Li-O₂ batteries decreases during cycling tests.^{8,35,38,42–52} It is important to note that RMs in Li-O₂ cells may undergo deactivation and shuttle reactions with the Li metal anodes during cycling.^{42–44} Thus, the stability of RMs in these systems is an important issue. In order to mitigate the possible side reactions of RMs, most approaches have been focused on prohibiting reactions of RMs with Li metal by surface treatment of the Li metal anodes or by prohibition of RMs crossover in the cells.^{42–52} However, reaching full stability of the Li anodes by any type of surface protection is questionable and prohibition of RM crossover in Li-O₂ cells is not an easy task, as was discussed in previous reports.^{47,52} Some papers have also reported on the detrimental effect of impurities such as trace water on the reaction mechanisms of RMs in Li-O₂ cells.^{38,39,53–58} There are also reports on the possibility of cathode passivation owing to side reactions of the RMs.^{42,47,52}

After reviewing the extensive accumulated literature related to Li-O₂ batteries, the importance of electro-catalysis in these systems by the RMs in solution phase is obvious. However, it seems that no systematic studies have examined the true suitability of RMs to Li-O₂ cells.

This work is aimed at examining selected RMs that can be considered as representing two classes: organic electrochemically active molecules and Li halides. It is believed that the selected RMs for the present study (tetramethyl-piperidinyloxy (TEMPO),^{8,35,42,59–62} tetrathiafulvalene (TTF),^{34,45,58,63–65} dimethylphenazine (DMPZ),^{36,46,47} LiBr,^{38,51,52,66,67} and LiI)^{37,43,44,48–50,53–57,68–76} are the most intensively studied RMs in Li-O₂ cells. Thereby, this study has a general importance for the field because of the scope of RMs that belong to several families of compounds.

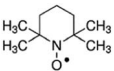
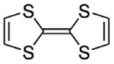
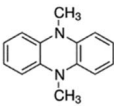
Table I shows the formulae of the selected RMs, their red-ox reactions and red-ox potentials, including appropriate references. All the systems were studied under nearly identical conditions (within acceptable experimental errors). The solution selected for this study comprised 1 M bis(trifluoromethane)sulfonimide lithium (LiTFSI) in dithyleneglycol dimethylether (DEGDME, diglyme). This solution is one of the most important for Li-O₂ cells because of its relatively acceptable compatibility with both the metal anode and the oxygen reduction products. It possesses a relatively high ionic conductivity and wide enough electrochemical window for properly testing the above-indicated RMs. It is important to note that DEGDME undergoes side reactions with the peroxide and superoxide moieties formed by oxygen reduction, especially when the highly electrophilic Li cations are present.^{77–79} Nevertheless, despite its reactivity in Li-O₂ cells, this solution is the most appropriate we have for emphasizing the intrinsic

limitations related to the RMs themselves. Each of the six solutions studied herein (the five containing RMs and the reference one) was investigated under four different conditions. We used cells with no separation between the anode and cathode compartments and cells in which the anode and cathode sides were separated by a Li-ion conducting membrane, as shown in Figure 1a. In the latter cells, there was no molecular transport or any crossover between the cathode and the anode compartments, as shown in Figure 1b. Both types of cells (loaded with the above six solutions) were tested under Ar and O₂ atmospheres. The electrochemical tool used was cyclic voltammetry (CV), as this is the most visual electrochemical technique for qualitative, comparative solution evaluations. UV-Vis spectrometry was used as an additional analytical tool. Important parameters that were varied herein included the RMs concentrations, potential windows, and scanning rates. This study also included a rigorous post-mortem analysis that was intended to discover which cell components are the most responsible for the degradation processes. The references we provide here show that all the RMs studied in the present work have been explored previously (see summaries of previous works in Tables II–VI, related to the five RMs). Nevertheless, the novelty of the present study lies in its reliable comparison of representative RMs and the ability to fully avoid complications arising from the Li anodes, and the strict conclusions about the relevance of these RMs for practical Li-O₂ batteries.

Experimental

Preparation of Li-O₂ batteries.—For the cathodes, gas-diffusion layer sheets (GDL, SGL, 35 BC) were punched into circular pieces of 1.4 cm in diameter and were dried at 180°C under vacuum for 3 d. 1 M bis(trifluoromethane)sulfonimide lithium salt (LiTFSI, 99.95%, Sigma Aldrich) in dithyleneglycol dimethylether (DEGDME, >99.5% anhydrous, Sigma Aldrich) was used as the electrolyte solution with and without the RMs (0.02 or 0.1 M): TTF (tetrathiafulvalene), TEMPO (tetramethylpiperidinyloxy), DMPZ (dimethylphenazine), LiBr (lithium bromide), and LiI (lithium iodide). The electrolytes were previously purified by molecular sieves (three times) and vacuum drying until the final water content was < 10 ppm, determined using Mettler-Toledo Karl-Fischer titration without exposure to ambient air. The home-made type Li-O₂ cells were assembled with the dried cathodes, dried glass fiber (GF/C, Whatman, 180°C under vacuum for 3 d), lithium metal anode (100 μm, Honjo), solid electrolyte (LICGC, Ohara), and different electrolytes in an Ar-filled glove box (water and oxygen contents were less than 0.1 ppm). The configurations for the single and bi-compartment cells (S.C. and B.C.) and detailed information about them is provided in Figure 1a. After the cells assembly, they were stabilized under O₂ atmosphere (1.0 bar) for 1 h before the relevant electrochemical tests. Closed coin

Table I. The formulae of the RMs used in this work, their red-ox reactions, and red-ox potentials.

Name	Structural formula	Redox reactions	Oxidation potential (vs Li/Li ⁺)	Reference
Tetramethylpiperidinyloxy (TEMPO)		TEMPO [•] → TEMPO + e ⁻ TEMPO → TEMPO ⁺ + e ⁻	E = 2.92 V E = 3.76 V	35, 60
Tetrathiafulvalene (TTF)		TTF → TTF ⁺ + e ⁻ TTF ⁺ → TTF ²⁺ + e ⁻	E = 3.44 V E = 3.75 V	34, 58
Dimethylphenazine (DMPZ)		DMPZ → DMPZ ⁺ + e ⁻ DMPZ ⁺ → DMPZ ²⁺ + e ⁻	E = 3.28 V E = 3.95 V	36, 80
Lithium bromide (LiBr)	LiBr	Br ⁻ → 1/3 Br ₃ ⁻ + 2/3 e ⁻ 1/3 Br ₃ ⁻ → 1/2 Br ₂ + 1/3 e ⁻	E = 3.57 V E = 4.05 V	38, 66
Lithium iodide (LiI)	LiI	I ⁻ → 1/3 I ₃ ⁻ + 2/3 e ⁻ 1/3 I ₃ ⁻ → 1/2 I ₂ + 1/3 e ⁻	E = 3.17 V E = 3.73 V	53, 72

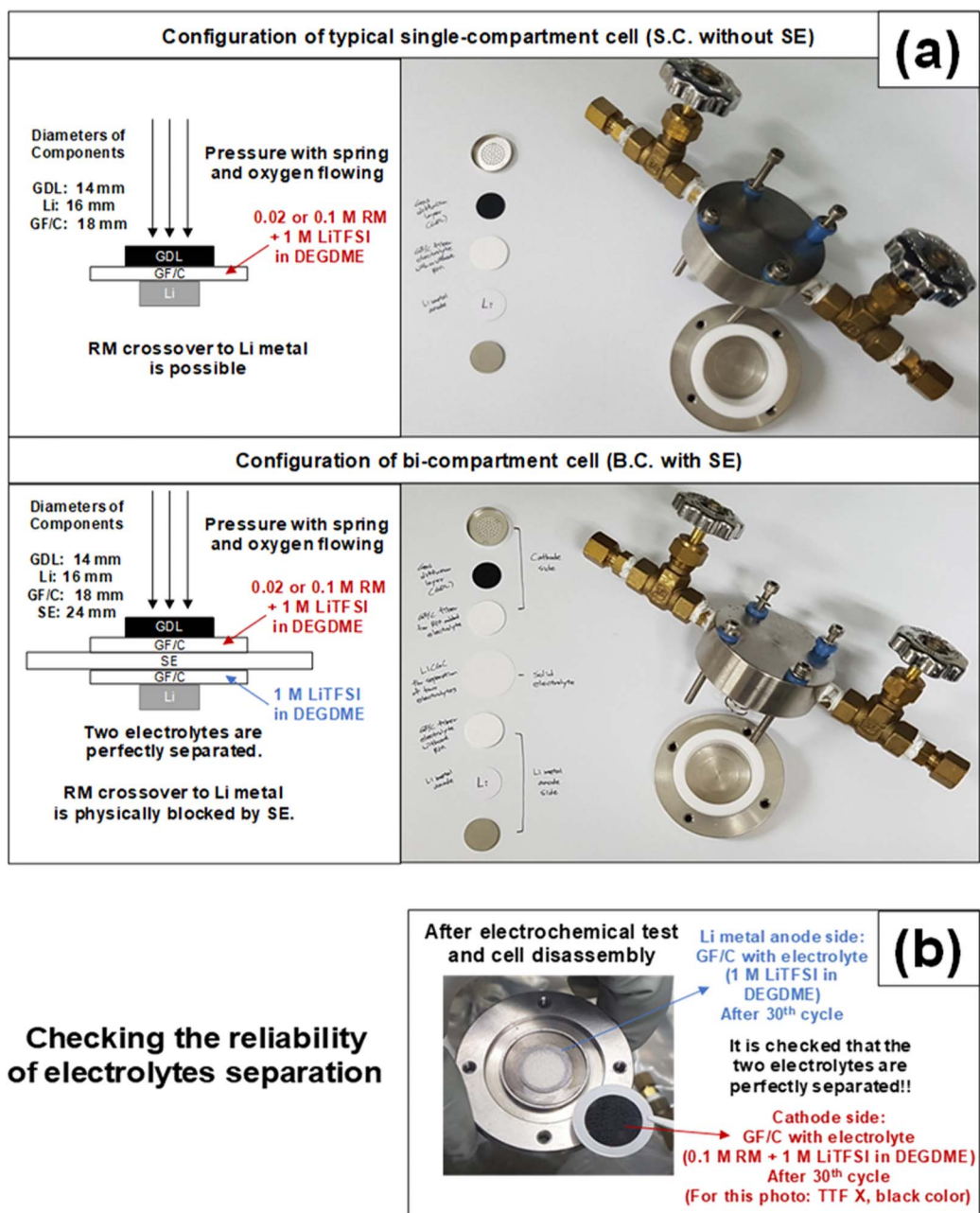


Figure 1. (a) Schematic images and photographs of the cells used for this study. The configurations of the single and bi-compartment cells (S.C. and B.C.) are described in detail. (b) Photograph of the bi-compartment cell after prolonged electrochemical testing, demonstrating appropriate separation between the cathode and anode sides with no reflections between them. Note the white-silver color of the Li metal anode. When there is no separation, the Li anode is colored and corroded.

cells without O_2 , for the experiments under pure Ar atmosphere, were fabricated with same procedure under an Ar-filled glove box. For each chart presented in this paper, the RM concentrations and cell types are indicated.

Characterization.—The electrochemical tests were conducted using the VMP3 from Biologic Instruments, set for cyclic voltammetric measurements with different scan rates (0.05, 0.1, and 1.0 $mV s^{-1}$) in different voltage windows (2.0–4.3, 2.3–4.0 V, 2.5–4.0 V, and respective redox potentials). The cathodes and discharge products were examined using field emission scanning electron microscopy (FE-SEM, SUPRA 55VP, Carl Zeiss) and high-resolution X-ray diffraction (HR-XRD, 9 kW, SmartLab, Rigaku) with the $Cu-K\alpha$ radiation source within $2\theta = 30.0^\circ$ – 60.0° at a scan rate of $1^\circ min^{-1}$. The solutions

after cell testing were collected and measured in an ultraviolet-visible spectrophotometer (UV-Vis, Lambda 650S). Before testing, the solutions were equally diluted by pure DEGME and UV-Vis spectra result from the solutes without that of DEGME solvent because DEGME is used as a sample for baseline.

Results and Discussion

Redox mediators in Li- O_2 batteries with single-compartment cells.—We concentrate herein in the response of the selected RMs in the two types of cells, under Ar and O_2 atmospheres as explained above. This work is the first one that focuses on the most commonly used RMs in Li- O_2 cells in a comparative study. There is extensive previous work on the five RMs selected for the present study. These works

Table II. Selected important works related to the use of TEMPO in Li-O₂ cells.

Redox mediator	Base solution	Cathode	Anode	V range	Purpose	Ref.
TEMPO, 10 mM	1.0 M LiTFSI in diglyme	Glassy carbon	Platinum	2.0–4.55 V	To exhibit TEMPO as effective RM	35
Nitroxides (TEMPO derivatives), 10 mM	1.0 M LiTFSI in diglyme	Ketjenblack	LiFePO ₄	2.0–4.5 V	For electrochemical characterization of nitroxides as RM	60
4-methoxy-TEMPO, 5 mM	0.5 M LiTFSI in DEME-TFSI	Glassy carbon	Platinum	2.3–4.5 V	To introduce 4-methoxy TEMPO for chemical oxidation of Li ₂ O ₂	61
TEMPO, 10–200 mM 4-methoxy-TEMPO, 100 mM	1.0 M LiTFSI in diglyme	Ketjenblack	Li metal LiFePO ₄	X	To separate the electrodes with SE for stable RM reaction	42
TEMPO, 50 mM	1.0 M LiClO ₄ in tetraglyme	MWCNTs	CPL coated Li metal	2.0–4.5 V	To protect the Li metal from the side reaction with TEMPO	8
TEMPO, 25 mM	20 mM DBBQ + 0.3 M LiClO ₄ in monoglyme	Carbon paper	LiFePO ₄	X	Pair of Soluble Redox Catalysts for Li-O ₂ batteries	62
TEMPO, 100 mM	100 mM DBBQ + 1.0 M LiTFSI in tetraglyme	Porous ATO	Li metal	X	Pair of Soluble Redox Catalysts with porous non-carbon cathode for Li-O ₂ batteries	59

Table III. Selected important works related to the use of TTF in Li-O₂ cells.

Redox mediator	Base solution	Cathode	Anode	V range	Purpose	Ref.
TTF, 5 mM	0.1 M TBAClO ₄ in DMSO	Gold	Platinum	1.75–4.25 V	To exhibit TTF as effective RM	34
TTF, 10 mM	0.5 M LiClO ₄ in DMSO	Ketjenblack or Gold	LiFePO ₄	2.0–4.2 V	To investigate the side reaction of TTF with porous carbon	63
TTF, 50 mM	1.0 M LiTFSI in tetraglyme	Platinum	Li metal	2.0–4.5 V	To exhibit the instability of TTF during cycles and results from LiFePO ₄	58
TTF, 5 mM	1.0 M LiClO ₄ in DMSO	Gold	LiFePO ₄	0–2.5 V (vs LiFePO ₄)	In-situ STEM analysis	64
TTF, 50 mM	1.0 M LiClO ₄ in DMSO	nanoporous graphene	Li metal	2.2–4.5 V	Synergy effect of TTF with nanoporous graphene	65
TTF, 1 mM	0.1 M LiPF ₆ in DMSO	GC/Au	Li metal	1.9–4.1 V	Confirming the redox catalytic effect of TTF on Li ₂ O ₂ decomposition	45

are summarized in Tables II–VI related to TEMPO, TTF, DMPZ, LiBr, and LiI, respectively. However, none of the previous studies focused on the intrinsic behavior of the RMs. Thus, although there are reports on the expected shuttle reactions of the RMs with the Li metal anodes in Li-O₂ cells, these works do not indicate whether this is the main problem of the RMs in these cells. There are recent papers using RMs in Li-O₂ cells containing protected Li metal anodes. However, there is no guarantee that any of the Li metal protection suggested can really avoid the expected shuttle mechanism. In this work, we could use “sterile” conditions that fully isolated the Li anodes, preventing them from influencing the cathode side. Hence, we could concentrate on other intrinsic problems related to the use of RMs in Li-O₂ cells and generalize them, thus being able to suggest more promising direc-

tions. In this respect, the fully comparative study conducted is very important because the conclusions are general, and thus, relevant to all the RMs examined. The starting point and background for this study is the information about the red-ox properties of the RMs, which are summarized in Table I.

Table I provides the main red-ox processes of the five RMs and their characteristic potentials, which are already known from previous studies.^{34–36,38,53,58,60,66,72,80} Figures 2 and 3 show representative CVs of the single-compartment cells under Ar atmosphere at two potential domains (2–4.3 V and 2.3–4 V vs. Li), loaded with the six solutions: the reference, 1 M LiTFSI/DEGDME, and the five solutions containing RMs. These figures display the 1st and the 30th CVs (consecutive repeated cycles) of the cells measured at 1 mV s⁻¹. Figure 3 relates

Table IV. Selected important works related to the use of DMPZ in Li-O₂ cells.

Redox mediator	Base solution	Cathode	Anode	V range	Purpose	Ref.
DMPZ, 10 mM	1.0 M LiTFSI in tetraglyme	Gold	Platinum	2.0–4.5 V	To exhibit DMPZ as selected RM based on energy level	36
DMPZ, 200 mM	1.0 M LiTFSI in diglyme	Carbon paper	Li metal	2.5–3.8 V 2.4–4.2 V	To prevent the side reaction of RM with Li metal by charged separator	46
DMPZ, 200 mM	1.0 M LiTFSI in tetraglyme	MWCNTs	Li metal	2.0–4.2 V	To optimize RM effect with Li metal protection by separation of electrodes with SE	47

Table V. Selected important works related to the use of LiBr in Li-O₂ cells.

Redox mediator	Base solution	Cathode	Anode	V range	Purpose	Ref.
LiBr, 50 mM	0.2 M LiTFSI in diglyme	Platinum	Li metal	2.0–4.2 V	To exhibit LiBr as RM without LiOH formation	38
LiBr, 10 mM	1.0 M LiTFSI in diglyme	Ketjenblack	Li metal	3.0–4.5 V	To exhibit LiBr as RM for OER and suppressing side reaction	66
LiBr, 50 mM	1.0 M LiNO ₃ in tetraglyme	Ketjenblack	Li metal	2.85–4.2 V	To reduce the polarization by Br ⁻ with protection of Li metal by NO ₃ ⁻	51
RuBr ₃ , 100 mM	1.0 M LiTFSI in DMSO	Carbon paper	Li metal	2.5–4.3 V	To exhibit the RuBr ₃ as bifunctional catalyst for Li-O ₂ batteries	67
LiBr, 100 or 500mM	1.0 M LiTFSI in diglyme	Carbon paper	GPDL coated Li metal	2.5–3.8 V	To increase the RM effect by optimization of RM condition and protection of Li metal	52

Table VI. Selected important works related to the use of LiI in Li-O₂ cells.

Redox mediator	Base solution	Cathode	Anode	V range	Purpose	Ref.
LiI, 10 or 50 mM	1.0 M LiTFSI in tetraglyme	Co ₃ O ₄ + Ketjenblack	Li metal	X	To enhance the battery performance using LiI with Co ₃ O ₄ catalyst	68
LiI, 50 mM	1.0 M LiTFSI in tetraglyme	Polydopamine-coated CNTs	Li metal	X	To enhance the battery performance using LiI with Polydopamine-coated CNTs	69
LiI, 50 mM	1 M LiTFSI in tetraglyme	CNT fibril	Li metal	X	To enhance the battery performance using LiI with ultralight cathode	70
LiI, 100 mM	1.0 M LiClO ₄ in DMSO	P50 carbon paper	Li metal	3.3–4.5 V	To exhibit photo-assisted charging in Li-O ₂ battery	71
LiI, 10 mM	0.2 M LiTFSI in tetraglyme	Platinum	Li metal	2.0–4.0 V	To confirm the side reaction of LiI to form LiOH in Li-O ₂ battery	53
LiI, 50 mM	0.25 M LiTFSI in monoglyme (DME)	rGO	Li metal	2.2–3.6 V	LiOH based Li-O ₂ battery with rGO	37
LiI, 5 mM	5 mM EV + 1.0 M LiTFSI in tetraglyme	Platinum	Li metal	2.4–4.0 V	Pair of Soluble Redox Catalysts for redox flow Li-O ₂ batteries	72
LiI, 50 mM	LiI decorated gel polymer (PP-PMS-TiO ₂ immersed in LiI + 1.0 M LiClO ₄ in tetraglyme)	RuO ₂ on rGO	Li metal	X	To exhibit combination effect of RM@GPE and RuO ₂ @RGO	73
InI ₃ , 16.7 mM	0.5 M LiClO ₄ in DMSO	MWCNTs	Li metal	X	To protect the Li metal by pre-deposited indium layer coming from InI ₃ RM	43
LiI, 500 mM	1.0 M LiTFSI in tetraglyme	doped carbon with nori biomass	Li metal	X	To enhance the battery performance using LiI with new type of doped carbon catalyst	74
LiI, 50 mM	0.25 M LiTFSI in monoglyme (DME) with H ₂ O	Ketjenblack	Li metal	2.0–4.2 V	To confirm the side reaction of LiI to form irreversible LiOH with water	54
LiI, 50 mM	1.0 M LiTFSI in tetraglyme/BuOH (1:1 v/v ratio)	Platinum	Li metal	2.0–4.0 V	To exhibit n-butanol can proper proton activity and promote the RM	75
LiI, 50 mM	1.0 M LiClO ₄ in tetraglyme	MWCNTs	Li metal	2.0–4.2 V	To prevent the side reaction of RM with Li metal by PU separator	44
CsI, 50 mM	0.5 M LiTFSI + 0.5 M LiNO ₃ in tetraglyme	PEDOT:PSS coated CNTs	Li metal	X	To hinder the growth of Li dendrite by the electrostatic shield effect of Cs ⁺ ions	76
LiI, 50 mM	1.0 M LiClO ₄ in tetraglyme	Porous TiN	Li metal	2.0–4.5 V	To prevent the side reaction of RM with Li metal by PU separator	48
LiI, 50 mM	LiI decorated gel polymer electrolyte	rGO	Li metal	X	To reduce the polarization with protection of Li metal	49
LiI, 2.5 mM, EVI ₂ , 2.5 mM	0.5 M LiTFSI in DME or DEGDME-DMSO (1:1 v/v)	Platinum	Platinum	2.0–4.5 V	To understand the battery chemistry in water contaminated Li-O ₂ batteries with LiI.	55
LiI, various concentration	LiTFSI in monoglyme (DME) with or without H ₂ O and KO ₂	vertically aligned few-walled CNTs	Li metal	X	To examine the role of LiI and related side reaction in different conditions	56
LiI, 10 or 1000 mM	LiI and/or LiTFSI in tetraglyme Concentration of LiI+LiTFSI: 1.0 M	Ketjenblack	Li metal	X	To exhibit the water can inactivates the catalysis of iodide to form LiOH	57
LiI(3-hydroxypropionitrile) ₂ (LiI(HPN) ₂), 100 mM	1.0 M LiTFSI in tetraglyme	Super P	Li metal	X	To improve the efficiency of I ⁻ with a high binding ability	50

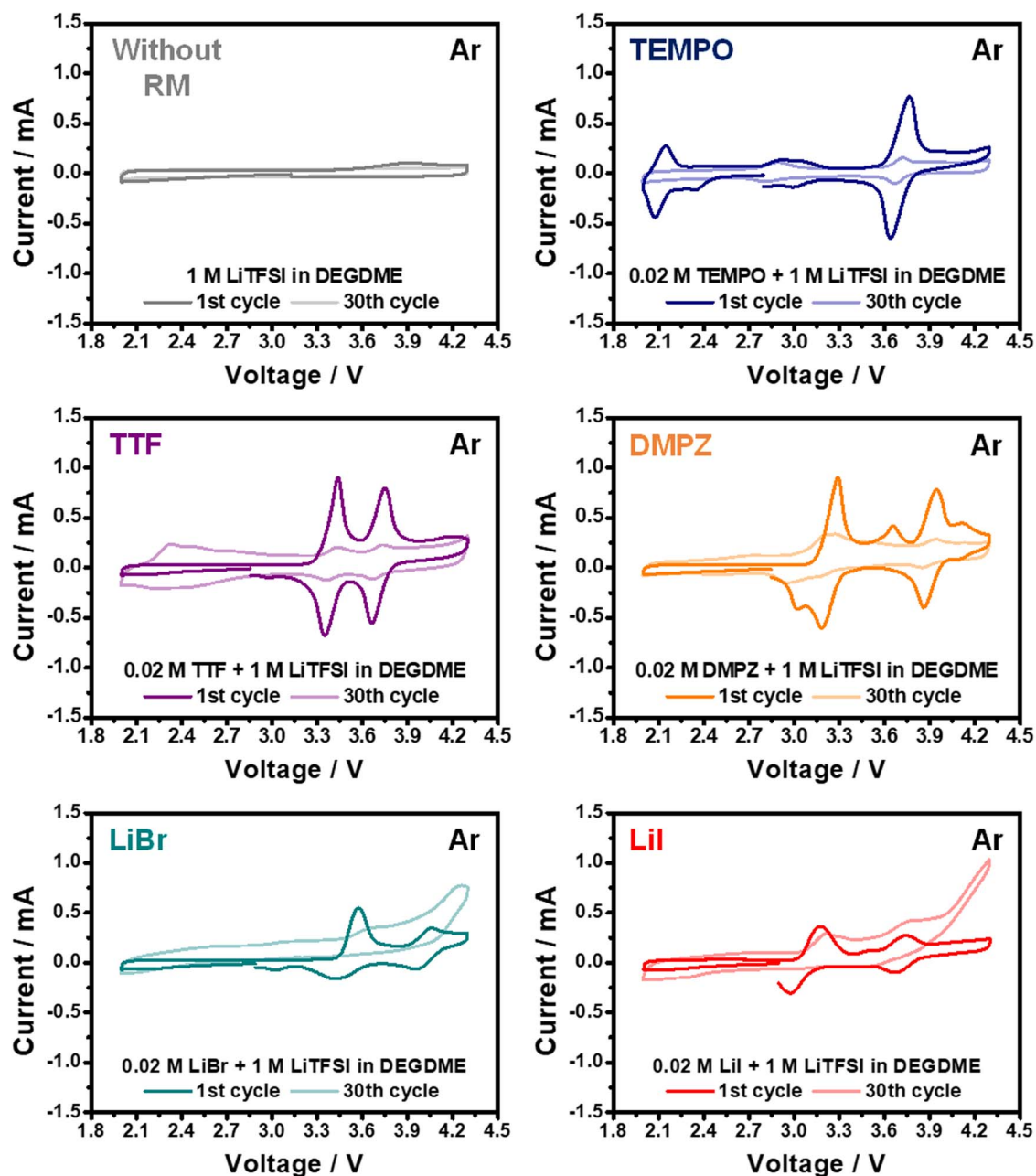


Figure 2. Comparative voltammetric charts of single-compartment cells (without SE), loaded with 1 M LiTFSI/DEGDME solutions (reference and with 0.02 M redox-mediators as indicated) showing the CVs of the 1st and the 30th cycles under Ar atmosphere with a scan rate of 1 mV s⁻¹ in the voltage range of 2.0–4.3 V.

to the practical potential window in which the RMs should play their role in Li-O₂ cells: 2.3–4.0 V. Within this potential domain, the oxygen evolution reaction (OER) should take place, aided by the catalytic activity of the RMs, because in these potentials both ether-based solutions and carbon substrates are anodically stable. In general, the CVs in Figures 2 and 3 reflect nicely the data appearing in Table I, showing two major red-ox processes for each of the RMs in the range 2.3–4.3 V vs. Li, while the voltammetric behavior of cells without RM is purely capacitive. For TTF, DMPZ, and Lil, both red-ox processes can catalyze the OER in these systems. (Of course, based on controversial opinions in previous reports, Lil has to be discussed further in order to determine which state is effective for Li₂O₂ decomposition as a redox mediator.)^{37,43,44,48–50,53–57,68–76} For TEMPO only the second (higher voltage) process is relevant and for LiBr only the first process (lower voltage) is relevant for OER in ether-based solutions, which anodic stability is limited to around 4.0 V vs. Li.

There are several interesting details in Figures 2 and 3:

1. The red-ox process of TEMPO around 2.8 V, related to reduction of its neutral state (not relevant to the OER in Li-O₂ cells), occurs at much lower capacity compared to its oxidation process (probably it involves only a partial electron transfer per molecule). Lowering the potential to 2.0 V enables completion of the reduction process of TEMPO by a pronounced reversible process occurring around 2.2 V (Figure 2).
2. The charts related to DMPZ show in fact four red-ox processes, two major and two minor. At high potential scanning rates or high concentrations (not shown herein), the CV response of DMPZ converges indeed to two observed red-ox processes with characteristic potentials that match the previously known red-ox response (Table I). These results reveal the nature of the red-ox processes of DMPZ, which occur by consecutive partial electron

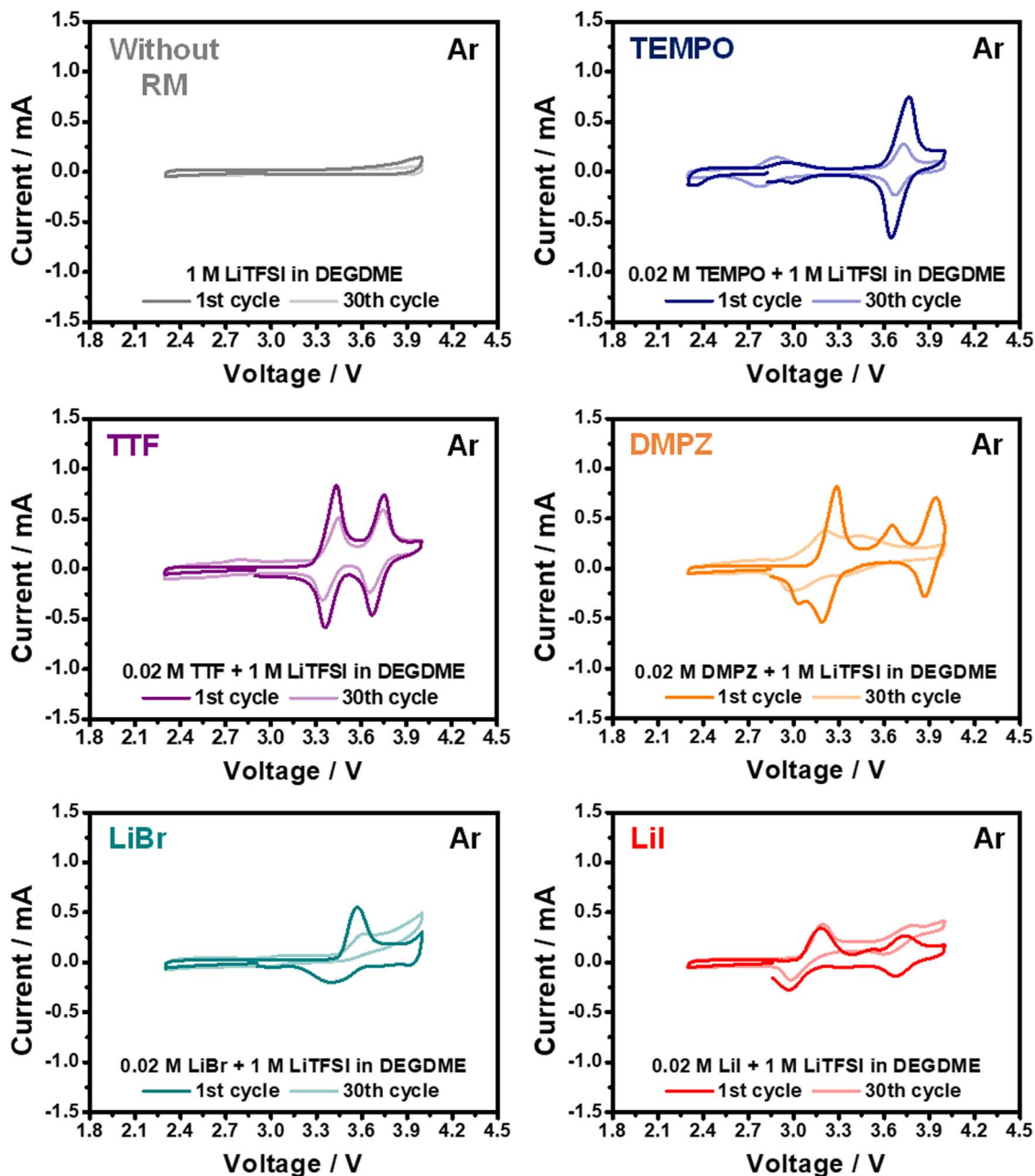


Figure 3. Comparative voltammetric charts of single-compartment cells (without SE), loaded with 1 M LiTFSI/DEGDME solutions (reference and with 0.02 M redox-mediators as indicated) showing the CVs of the 1st and the 30th cycles under Ar atmosphere with a scan rate of 1 mV s⁻¹ in the voltage range of 2.3–4.0 V.

transfers (relevant to both the anodic and cathodic processes). This complexity of the electrochemical behavior of DMPZ should not affect its functionality as RM of the OER in Li-O₂ cells, as all of its anodic processes in the potential range 2.3–4.0 V can catalyze very well the oxidation of Li₂O₂ to molecular oxygen.

- Contracting the electrochemical window (Figure 3) does not change the response of TEMPO, TTF, and LiI solutions. However, limiting the upper potential to 4.0 V excludes the 2nd process related to LiBr (Br₃⁻ → Br₂) and the minor process of DMPZ that occurs above 4.0 V (see Figure 2). The low potential process of TEMPO is excluded when the lower potential limit is set to 2.3 V.
- The most important result, which is clearly seen in Figures 2 and 3, is the pronounced decrease in the voltammetric currents of all the RM processes upon cycling. The currents gradually decrease during cycling, clearly reflecting degradation of the electrochemical response of the RMs, even in the absence of oxygen and

formation of highly reactive superoxide and peroxide moieties in the cells.

Figure 4 shows the comparative CV responses of these cells loaded with the six solutions under pure O₂ atmosphere in the potential domain 2.3 – 4 V, at 1 mV s⁻¹. The concentration of the RMs in these experiments was high (0.1 M).

The voltammetric response of the cells loaded with the reference solution reflects the oxygen reduction reaction (ORR) at potentials below 2.7 V, with the corresponding OER along all the voltage range > 3.0 V. The corresponding charges of the ORR and OER of these cells (no RMs) are comparable. Upon cycling, the currents related to the ORR and OER diminish very pronouncedly. The instability of these systems is obvious and impressive. The electrochemical responses of the cells containing RMs at relatively high concentration reflect two parallel processes: the intrinsic, nearly undistorted, electrochemical

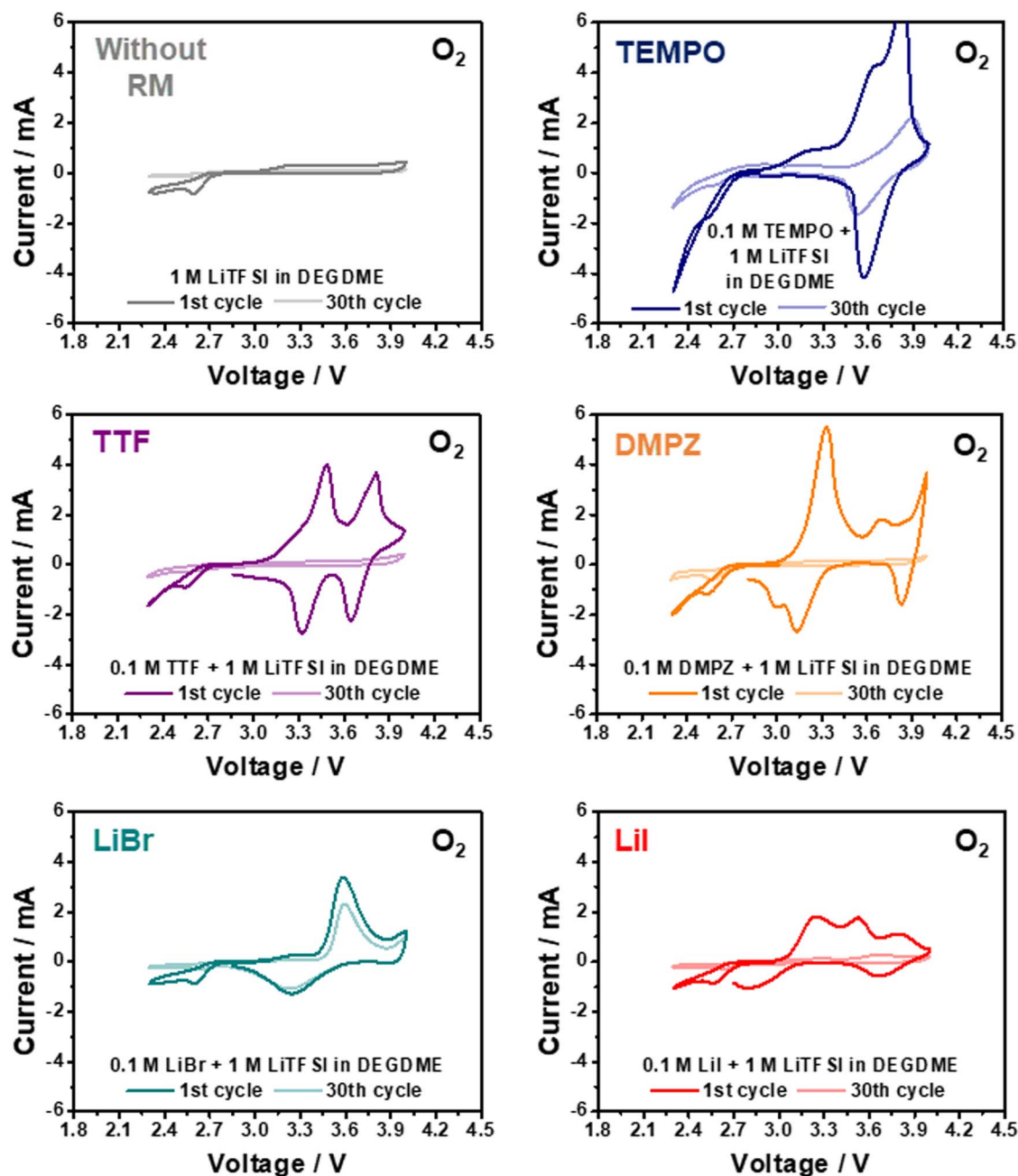


Figure 4. Comparative voltammetric charts of single-compartment cells (without SE), loaded with 1 M LiTFSI/DEGDME solutions (reference and with 0.1 M redox-mediators as indicated) showing the CVs of the 1st and the 30th cycles under O₂ atmosphere with a scan rate of 1 mV s⁻¹ in the voltage range of 2.3–4.0 V.

reactions of the RMs under O₂ atmosphere similar to those presented in Figures 2, 3 and the oxygen red-ox reactions – its reduction to Li₂O₂ and oxidation of the Li-peroxide in the charging process, catalyzed by the RMs. The mediated OER is clearly distinctive in solutions containing TEMPO, as it has an additional anodic peak or shoulder around 3.6 V. With the other RMs, the catalyzed OER response is merged, superimposed with the intrinsic anodic responses of these systems. All the cells undergo degradation upon repeated cycling, as reflected by the decaying voltammetric currents. These degradation processes are affected by the potential windows and the nature of the RMs. A detailed discussion on the fine details of the voltammetric response of the six systems presented in Figures 2–4 is not important at this point, because all the measurements presented in these figures are in fact an introduction to the main part of the study, which is described below.

Until now, most studies related to Li-O₂ cells were carried out in single-compartment cells in which the reactions of the cells were highly influenced by detrimental reflections and ‘cross-talking’ between the cathodes and the highly reactive Li metal anodes. The solution species in such cells are exposed to inevitable side reactions with the Li anode and with the highly basic and nucleophilic superoxide and peroxide species formed by oxygen reduction. These species formed on the cathode side obviously migrate/diffuse to the Li side and attack the active metal and its passivating surface films. Under this situation, it was impossible to understand the degradation processes of the RMs in these cells and properly isolate the various detrimental effects, in order to judiciously alleviate them. Hence, it is critically important to conduct a systematic research on Li-O₂ battery systems with bi-compartment Li-O₂ cells, in which the anode and the cathode sides are fully separated, and thus, with no mass transport except

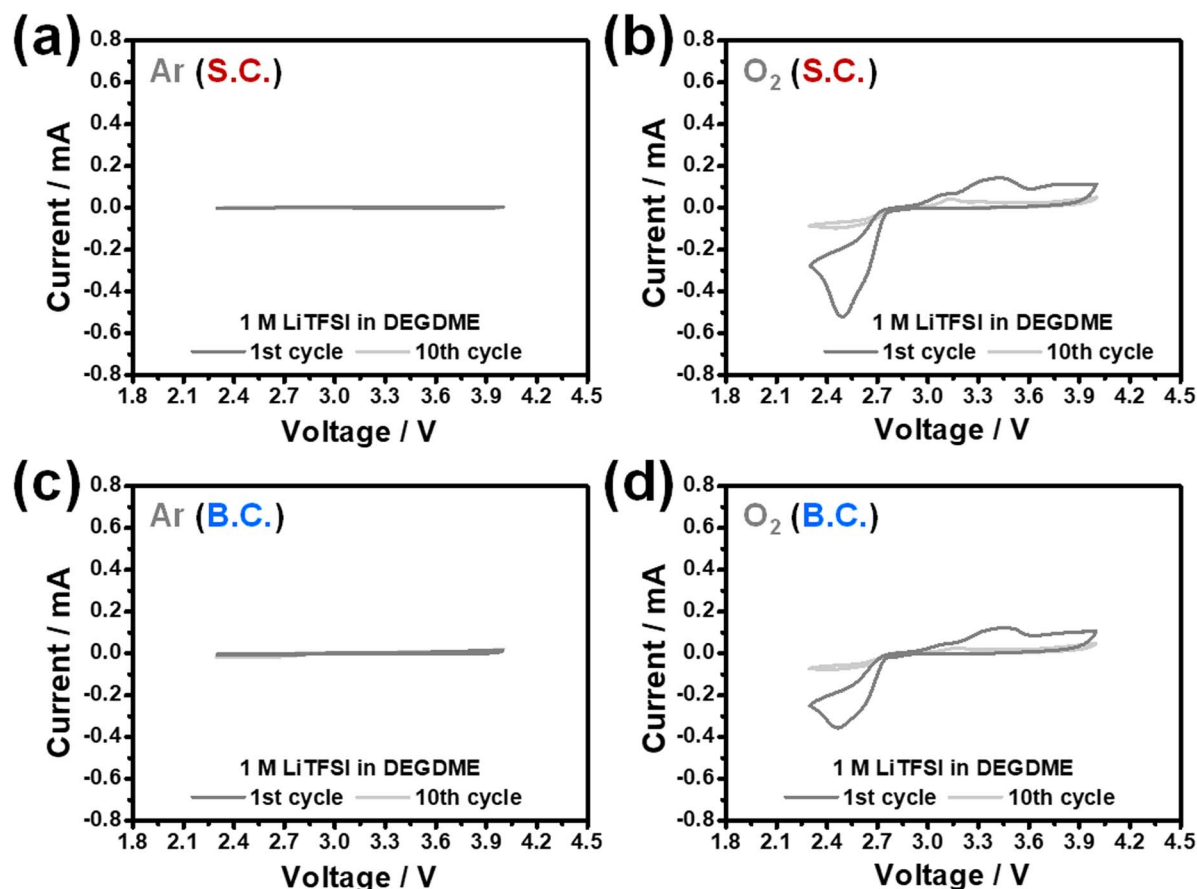


Figure 5. Comparative voltammetric charts of single (without SE) and bi-compartment cells (with SE), loaded with 1 M LiTFSI/DEGDME solutions (no RM present) under Ar and O₂ atmospheres as indicated, showing the first and 10th CV cycles; 0.05 mV s⁻¹, 2.3–4.0 V vs. Li. (a) and (b): single-compartment cells; (c) and (d): bi-compartment cells. (a) and (c): Ar atmosphere; (b) and (d): O₂ atmosphere. S.C. and B.C. indicate single or bi-compartment cells, respectively.

Li ions. While such cells may not have a practical meaning, they could be highly useful for performing systematic studies that identify all the various detrimental processes in these systems, and consequently for selecting better components for Li-O₂ batteries.

All the six solutions explored herein were studied in the bi-compartment cells described in Figure 1 under Ar and O₂ atmospheres. We utilized for these studies practical RM concentrations (0.02 M) and sufficiently slow potential scanning rates (0.05 mV s⁻¹). Thus, the electrochemical response of the cells could not be hindered by polarization over-potentials owing to concentration gradients of Li ions near the separating membranes of the cells. The comparative results for each of the solutions are described below. Please note that all the experiments were nearly identical, and thus, the I vs E responses of the various experiments (with all the solutions) are shown on identical scales, which allows a very meaningful (semi-quantitative) comparison.

Cyclic voltammetry tests using bi-compartment cells with TEMPO.—Figure 5 shows very similar responses of the single-compartment and bi-compartment cells for both Ar and O₂ atmospheres. The expected ORR and OER responses are clearly seen in charts b and d. The striking result here is the fact that after 10 cycles the ORR and OER capacities are only a few percent of those in the first cycle, even with the measurements in the bi-compartment cell. This means that there is a major capacity fading mechanism related only to the cathode side. Note that in these voltammetric measurements the cells undergo deep ORR and OER processes, and therefore, the degradation is faster compared to galvanostatic experiments in which the ORR and OER capacities are limited.^{2,38,39,53} These results

are well explained by previous studies, which showed that glyme solvents are attacked in the Li-O₂ cells by the superoxide and peroxide species formed by oxygen reduction.^{29–33,81} These side reactions are especially effective owing to the presence of the electrophilic Li ions in the solutions.⁸² In previous studies, we could suggest mechanisms for the side reactions based on the products analysis.^{83,84}

Figure 6 provides similar charts to those of Figure 5 related to similar experiments with solutions containing 0.02 M TEMPO. Note that in the potential range used in these measurements only the red-ox process of TEMPO, around 3.6 V (relevant to the OER), occurs. These charts show three important results:

1. The electrochemical response of the cells is very pronounced under O₂ atmosphere, compared to the response of the solutions under Ar atmosphere and compared to the ORR and OER in solutions without TEMPO (Figure 5), which reflects the effectiveness of TEMPO as a RM. It is important to note that in contrast to the response presented in Figure 4 and (relatively fast potential scanning rate), in these experiments, owing to the slow potential scanning rate, the red-ox mediation of the OER by TEMPO is so effective that almost no cathodic peaks for TEMPO⁺ reduction appear.
2. A pronounced decrease in the ORR and OER capacity is observed even after 10 cycles. This reflects the previously discussed degradation mechanisms, which belong solely to the cathode side in these systems.
3. Even under Ar and full separation between the anode and cathode side without any detrimental effect of the oxygen reduction species (Figure 6c), the electrochemical response of the TEMPO pronouncedly decreases after 10 consecutive cycles.

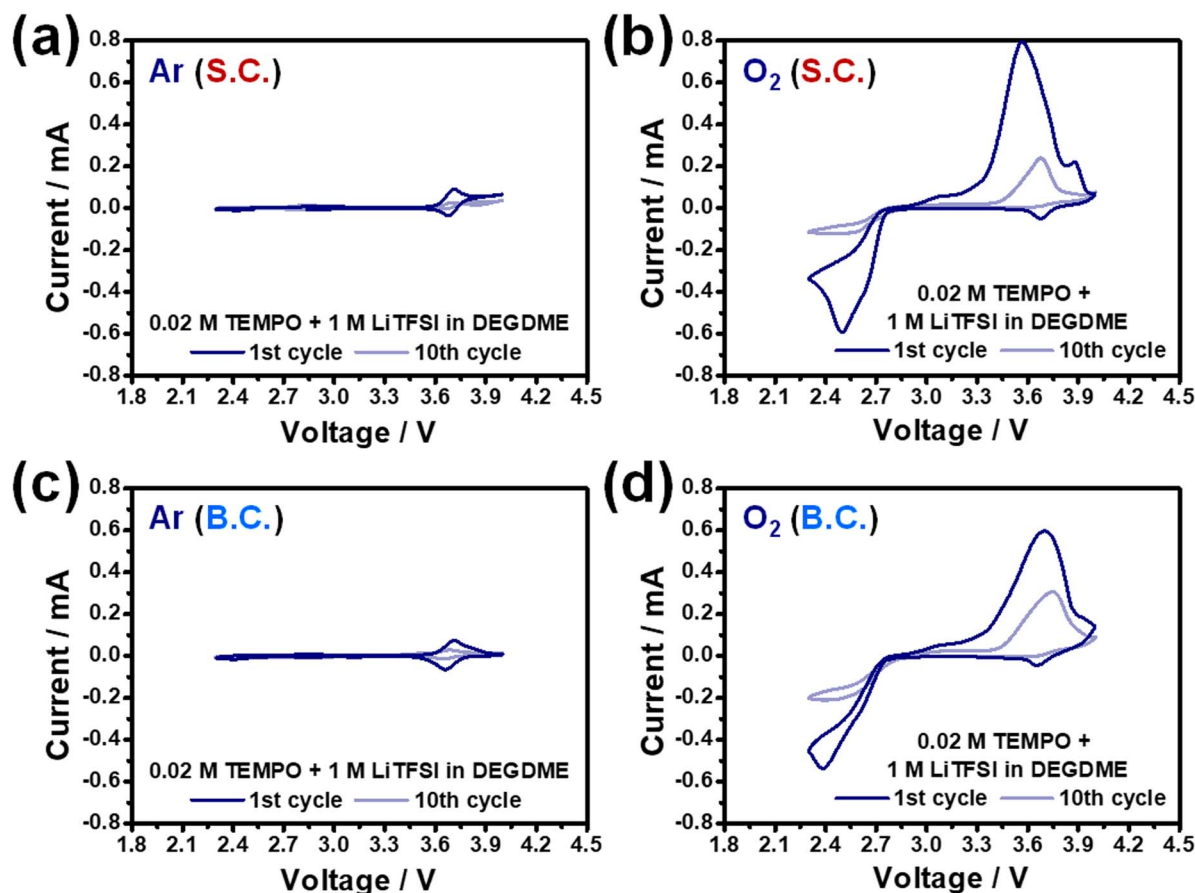


Figure 6. Comparative voltammetric charts of single (without SE) and bi-compartment cells (with SE), loaded with 1 M LiTFSI/DEGDME solutions containing 0.02 M TEMPO under Ar and O₂ atmospheres as indicated, showing the first and 10th CV cycles; 0.05 mV s⁻¹, 2.3–4.0 V vs. Li. (a) and (b): single-compartment cells; (c) and (d): bi-compartment cells. (a) and (c): Ar atmosphere; (b) and (d): O₂ atmosphere. S.C. and B.C. indicate single or bi-compartment cells, respectively.

It is very difficult to attribute the decrease in the electrochemical response presented in Figure 6c to the Li side, because Li anodes can be cycled reversibly in LiTFSI glyme solutions many dozens of cycles, especially as the anodes in these cells contain a large excess of lithium. Hence, we have to conclude that TEMPO undergoes degradation in these cells owing to intrinsic mechanisms. The exploration of these mechanisms is beyond the scope of the present work.

Analysis of deactivation of the redox mediators.—In parallel to the systematic electrochemical measurements, the electrolyte solutions and electrodes from cycled bi-compartment cells containing TEMPO were analyzed by spectroscopy, microscopy, and XRD. UV-Vis measurements were carried out with the electrolyte solutions after the 1st and 30th cycles and with the reference solution before cycling (Figure 7a). The GF/C fibers containing TEMPO from the cathode side were recovered (their contact with the Li metal was blocked by the solid electrolyte separator) and photographed (Figure 7b). Then they were diluted with pure DEGDME solvent in order to prepare the solution samples for UV-Vis measurements. In addition to UV-Vis, analyses of the solution samples by NMR and FTIR spectroscopies were also carried out, but they were not conclusive for detection of TEMPO degradation products owing to the low concentration of RM compared to that of solvent and Li salt. The spectral studies carried out herein were in line with previous studies by Janek et al., who studied extensively the use of TEMPO as an RM in Li-O₂ cells.⁴² The UV-Vis analysis confirmed that the peak related to TEMPO was maintained after discharge. After charging (1st cycle), the UV-Vis spectrum changed, as expected, owing to the conversion of TEMPO to its oxidized form (blue line in Figure 7a). This response was well documented in the previous study by Janek et al.⁴² However, the

UV-Vis spectra of the deactivated electrolyte solution after 30 cycles (green line in Figure 7a) showed apparently different peaks at < 350 nm which should be attributed to deactivated form of TEMPO, different from the known spectra of TEMPO and TEMPO⁺. This difference in the UV-Vis spectroscopic results can be easily verified with a naked eye by looking at the photographs of the separators taken from cycled cells (Figure 7b) as the corresponding wavelength region belongs to visible light. The pristine electrolyte solution containing TEMPO is reddish. It becomes yellow when TEMPO⁺ is formed by charging. After 30 cycles, the electrolyte solution became colorless. As demonstrated by the SEM and XRD studies (Figures 7c and 7d, respectively), after 30 cycles the cathodes retain their morphology and structure despite the pronounced deactivation of the electrochemical response. These findings mean that the deactivation is related to changes in the solution and not in the cathode.

Disassembling–reassembling experiments to check the route of deactivation of TEMPO.—In order to clarify further the reasons for the deactivation of the cells presented in Figure 6, we conducted a series of experiments with cells that were cycled, disassembled, and re-assembled with fresh components and measured again. This work is summarized in Figure 8, which presents descriptions (by sub images) of the disassembling–reassembling experiments (Figure 8a) and the relevant electrochemical CV data (Figure 8b). After eliminating the possibility of deactivation of TEMPO owing to reactions with the lithium metal anode, by using the bi-compartment cells, it is clear that the deactivation of TEMPO occurs at the cathode side. As explained above (discussion related to Figure 7), there are two main possible reasons for the deactivation of TEMPO (as reflected by the decrease in the voltammetric response of the cells upon cycling). One reason may

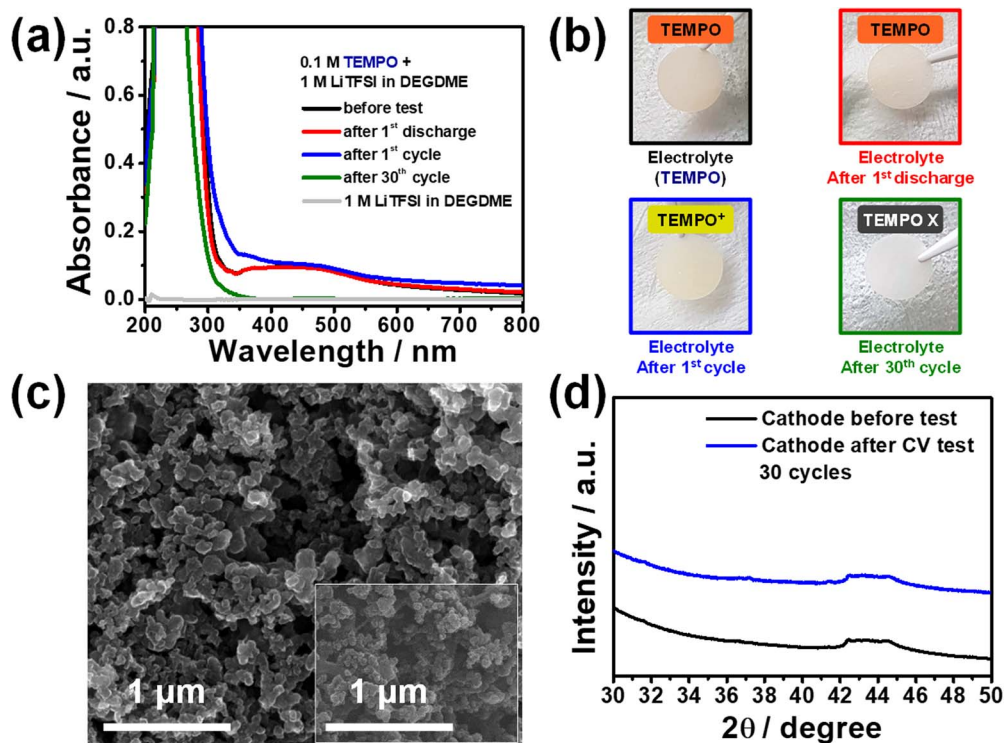


Figure 7. (a) UV-Vis solution spectra and (b) photographs of the separators soaked with the electrolyte solution containing TEMPO at different conditions, before the electrochemical testing, after 1st discharge, after 1st cycle, and after 30 CV cycles in bi-compartment cells under O₂ atmosphere. The solution composition was 0.1 M TEMPO + 1 M LiTFSI in DEGDMC, potential range was 2.5–4.0 V, and scanning rate of the CVs was 0.1 mV s⁻¹. (c) SEM and (d) XRD data for a cathode before and after 30th CV cycles. The inset image in the SEM image is a SEM micrograph of a pristine cathode.

be the decomposition of TEMPO (and/or TEMPO⁺) on the porous carbon cathode (even in the absence of oxygen species). The other reason may be cathode passivation owing to blockage by side reactions products. The experiments described in Figure 8 intended to clarify these points.

Bi-compartment cells with solution containing TEMPO and solution without TEMPO underwent 30th CV cycles (marked as ① in Figure 8a). The relevant voltammetric chart that shows the gradual deactivation of TEMPO in the cells is presented in Figure 8b (①). Then, the cells were disassembled and their components were re-assembled with new parts in four routes. In route ② (Figure 8a left), the used Li metal anode + electrolyte solution were assembled in a cell with a fresh cathode followed by cycling. In route ②' (Figure 8a left) the used electrolyte solution was assembled with a fresh cathode and Li metal anode followed by cycling. Both cycled solutions in these experiments contained initially active TEMPO. Figure 8b presents the relevant voltammetric charts of these reassembled cells. These charts exhibit very low activity of residual TEMPO in the cells, as reflected by the low currents. In route ③ (Figure 8a, right), a cathode cycled in a cell containing TEMPO (that showed a pronounced deactivation) was reassembled in a new cell containing fresh electrolyte with active TEMPO followed by cycling. In route ③', the cathode cycled in a cell containing solution without TEMPO was reassembled in a fresh cell followed by cycling. The relevant voltammetric charts are shown in Figure 8b (③ and ③'). These charts clearly show that the behavior of fresh cells is similar to that shown in chart ①, which means that the cathodes in these cells are not the reason for the deactivation of cells containing TEMPO. The huge OER peak at the first cycle in Figure 8b (③) results from the drastic decomposition of Li₂O₂ discharge products, which were formed on the cathode in the previous cell using an electrolyte solution without TEMPO. This huge peak demonstrates the effect of TEMPO as an RM on a fast decomposition of the Li₂O₂ discharge product.

Hence, the results of the sets of experiments described in Figures 7 and 8 converge to the clear conclusion that TEMPO in these cells loses its red-ox activity during cycling, because of some reactions in the solution phase. A detailed study of the TEMPO side reactions in these solutions and cells is beyond the scope of this work. What is important for the present study = is the conclusion about the intrinsic deactivation route of TEMPO owing to the detrimental reactions in these cells, even without any contact with the Li metal anodes.

Other redox mediators.—As seen in Figure 9a, at slow enough scanning rates, the electrochemical response of TTF in a single-compartment cell includes a pronounced shuttle reaction in which the oxidized TTF is continuously reduced on the Li anode (owing to a fast crossover of all solution species), and thus, the CVs of these cells do not show cathodic peaks (as was demonstrated at high scanning rates). As presented in Figure 9c, in bi-compartment cells (full anode/cathode separation) the shuttle reactions are fully avoided and the usual response of TTF is seen, namely, two sets of peaks reflecting the consecutive red-ox processes of TTF that characterize the CV response. As presented in Figures 9b and 9d, in the presence of oxygen the picture changes completely. At the slow scanning rates, oxidation of the Li₂O₂ formed by oxygen reduction becomes the dominant anodic reaction. Therefore, the voltammetric response of both single and bi-compartment cells does not include reduction peaks of oxidized TTF (as seen in Figure 9c), because any oxidized TTF reacts faster with the Li₂O₂ deposits than on the electrodes during the cathodic potential scans. In a very similar manner to the cells containing TEMPO, all the cells that contained TTF showed a very pronounced decay in their electrochemical response after 10 slow cycles. Highly interesting is the decay of the electrochemical response of the bi-compartment cells under Ar atmosphere. This means that TTF suffers from intrinsic electrochemical instability in the ether-based electrolyte

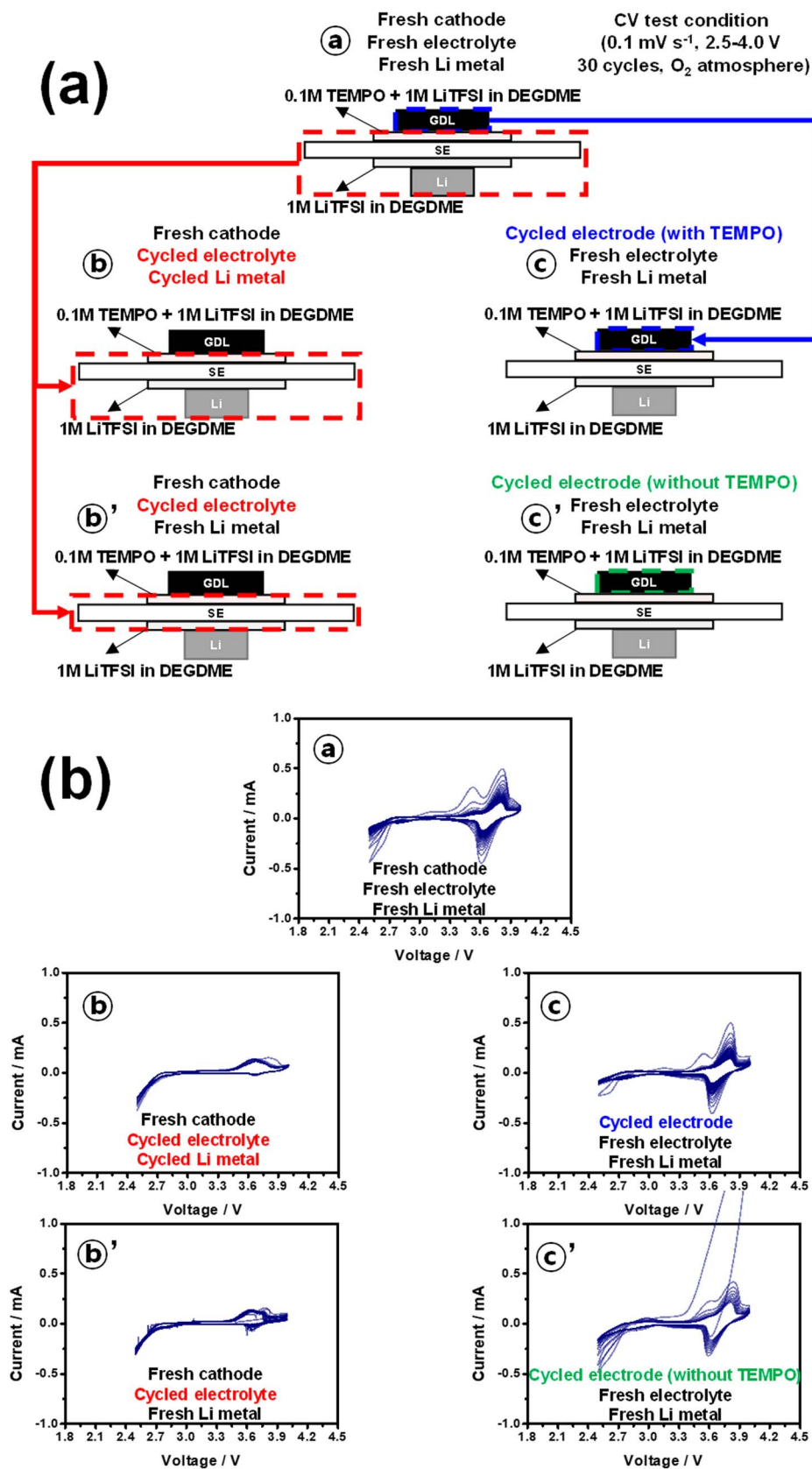


Figure 8. (a) Schematic description of the disassembling and re-assembling of cells with fresh components for retesting (bi-compartment cells containing TEMPO as the RM). (b) Voltammetric charts of the cells tested in this experimental part of the study. 1 M LiTFSI/DEGDM solution containing 0.1 M TEMPO, 0.1 mV s⁻¹, 2.5-4.0 V, 30 cycles, O₂ atmosphere. Profiles of first and last cycles are marked as black and red lines.

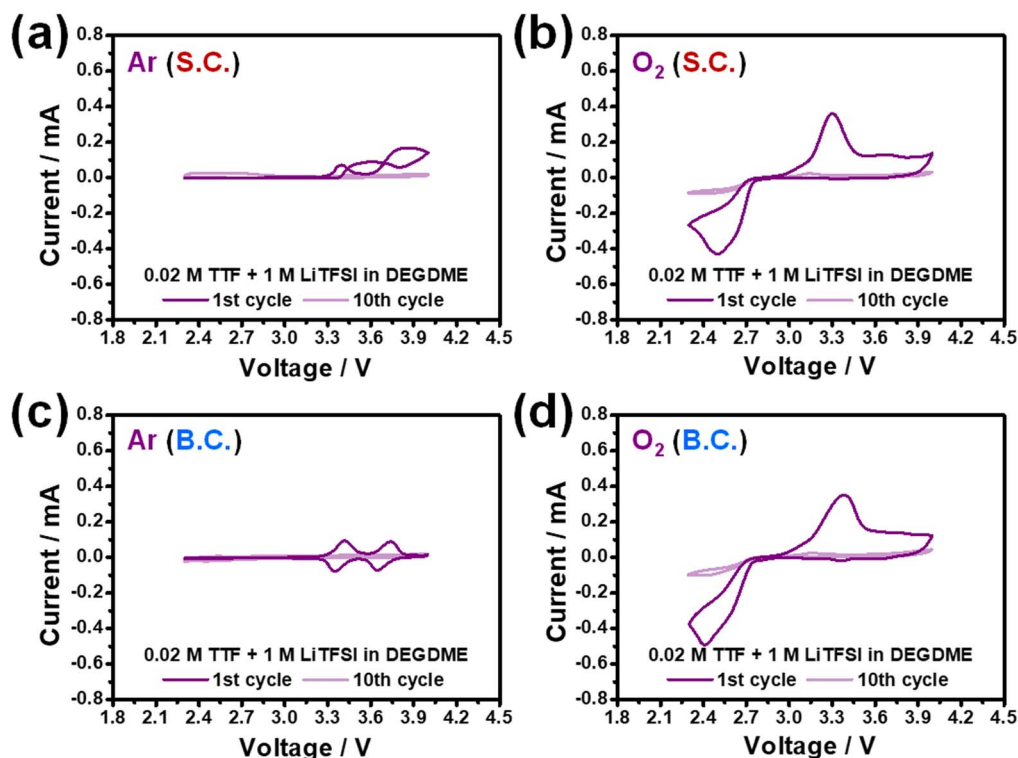


Figure 9. Comparative voltammetric charts of single (without SE) and bi-compartment cells (with SE), loaded with 1 M LiTFSI/DEGDME solutions containing 0.02 M TTF under Ar and O₂ atmospheres as indicated, showing the first and 10th CV cycles; 0.05 mV s⁻¹, 2.3–4.0 V vs. Li. (a) and (b): single-compartment cells; (c) and (d): bi-compartment cells. (a) and (c): Ar atmosphere; (b) and (d): O₂ atmosphere. S.C. and B.C. indicate single or bi-compartment cells, respectively.

solution with Li salt within the potential window relevant for Li-O₂ cells (2.3–4.0 V vs. Li).

Figure 10 presents the behavior of DMPZ solutions in single and bi-compartment cells, showing similar data to that in Figures 6 and 9. These solutions exhibit very similar trends to those of TEMPO and TTF: a shuttle behavior under Ar atmosphere in single-compartment cells and dominance of the ORR and DMPZ mediated OER in the O₂ atmosphere (which hinders the intrinsic electrochemical response of the DMPZ when the potential scanning rates are slow enough, as explained above). Although DMPZ was selected after considering that its unique electronic structure is very suitable for an effective oxidation of Li₂O₂ at relatively low potential,³⁶ we found in this study that it is intrinsically unstable within the potential domain of the ORR and OER in ether-based electrolyte solutions with Li salt. Hence, the notion that “the OER mediator is not consumed in the reaction, even if the addition of a small amount of OER mediator in the electrolyte can, in principle, complete the charging reaction”⁸¹ seems to be incorrect in practical approaches to the three organic RMs studied herein, owing to the severe decomposition issues of TEMPO, TTF, and DMPZ upon any practical operation of Li-O₂ batteries.

Figure 11 provides the results of post-mortem analyses of bi-compartment cells that contained TTF and DMPZ solutions (a and b, and c and d, respectively) and were cycled under an O₂ atmosphere. The solutions before and after the processes (as indicated) were measured by UV-Vis spectroscopy, and the spectral charts are shown in Figures 11a and 11c (TTF and DMPZ, respectively). Photographs of the GF/C fibers (their contact with Li metal was blocked by the solid electrolyte separator) taken from the cathode side in the cells are presented in Figures 11b (TTF) and 11d (DMPZ). The results presented in Figure 11 are very similar to the results presented above in Figure 7, related to cells and solutions containing TEMPO. The changes in the

spectra of the solutions and the colors of the separators soaked with solutions after cycling are fully in line with the electrochemical data presented in Figures 9 and 10. This very clearly reflects the changes in the solution compositions owing to deactivation of the RMs during cycling, regardless of side reaction with the Li metal anode.

Figures 12 and 13 present the results of cells and solutions containing LiBr and LiI, respectively, showing data similar to that presented in Figures 6, 9, and 10 related to the organic RMs. Both Figures 12a and 13a, related to single-compartment cells under Ar, exhibit the expected shuttle reactions of the halides red-ox couples in the first cycle. Figure 12a shows also pronounced anodic currents, which increase from cycle to cycle. These high anodic currents reflect a pronounced corrosion of the cells owing to interactions of the bromine species in solutions with the metallic cells’ components (see further discussion related to Figure 14). These corrosion phenomena are inhibited under the O₂ atmosphere (see Figure 12b), probably owing to passivation of the metallic parts of the cells by reactions with oxygen species. It is interesting to realize in Figures 12c and 13c (bi-compartment cells, Ar atmosphere) that the voltammetric response of both halides shows only anodic currents, and cathodic processes are not observed. This observation is explained by the relatively slow kinetic of the halides red-ox reactions. The separator in the bi-compartment cells further slows down their electrochemical response. Therefore, upon the anodic potential scans, only part of the Br⁻ or I⁻ anions in the cells are oxidized. Hence, the oxidation reactions continue during the cathodic scans, because the relevant potentials are high enough for oxidation of the halides. This continuous oxidation hinders possible minor reduction processes of the Br₃⁻, I₃⁻, and I₂ species, which are formed during the anodic scan. Figures 12b and 12d, and 13b and 13d (O₂ atmosphere) show a clear deactivation of the cells, which is less pronounced compared to the cells with organic RMs.

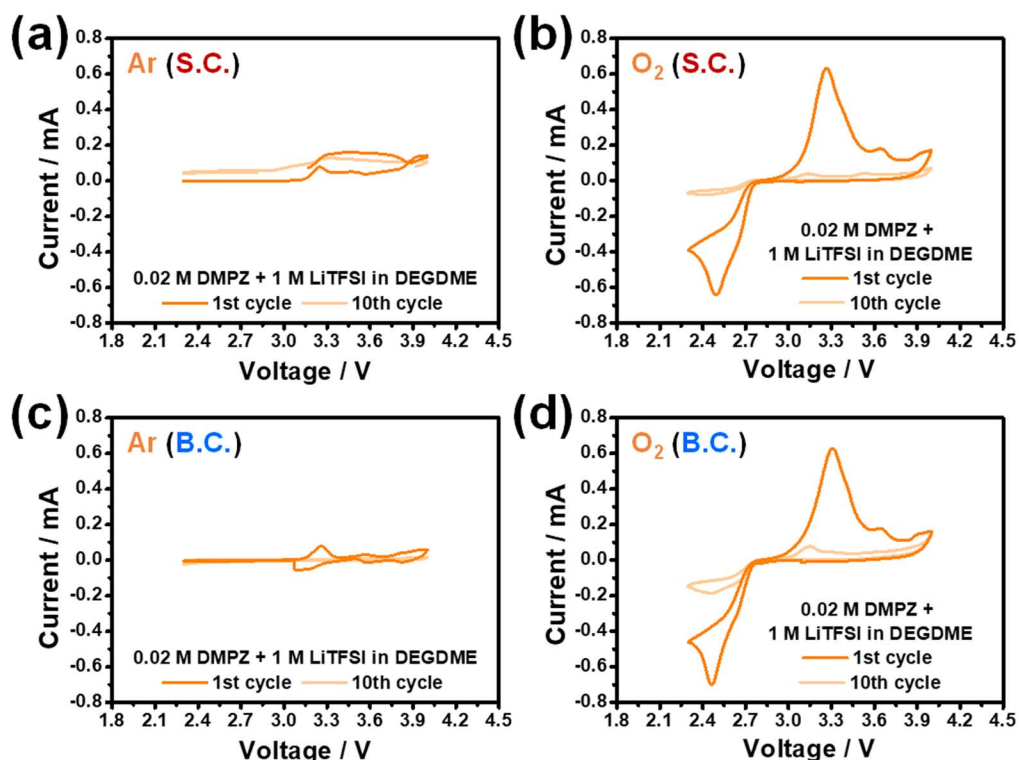


Figure 10. Comparative voltammetric charts of single (without SE) and bi-compartment cells (with SE), loaded with 1 M LiTFSI/DEGDME solutions containing 0.02 M DMPZ under Ar and O₂ atmospheres as indicated, showing the first and 10th CV cycles; 0.05 mV s⁻¹, 2.3–4.0 V vs. Li. (a) and (b): single-compartment cells; (c) and (d): bi-compartment cells. (a) and (c): Ar atmosphere; (b) and (d): O₂ atmosphere. S.C. and B.C. indicate single or bi-compartment cells, respectively.

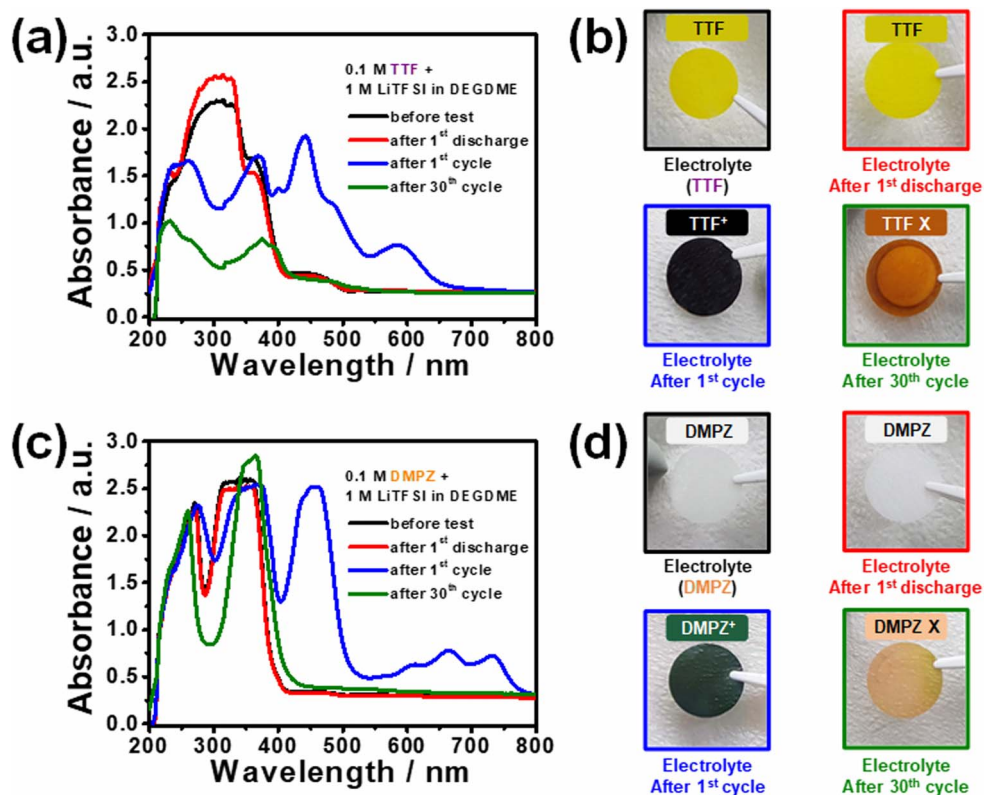


Figure 11. (a) UV-Vis solution spectra and (b) photographs of the separators soaked with the electrolyte solution containing TTF at different conditions; before the electrochemical testing, after 1st discharge, after 1st cycle, and after 30 CV cycles in bi-compartment cells under O₂ atmosphere. The solution composition was 0.1 M TTF + 1 M LiTFSI in DEGDM. The potential range was 2.5–4.0 V and the scanning rate of the CVs was 0.1 mV s⁻¹. Charts (c) and (d) provide similar data from identical experiments, with solutions containing 0.1 M DMPZ as indicated. The pronounced changes in color of the separators soaked with the cycled solutions are in line with the UV-Vis spectra, reflecting the instability of these systems.

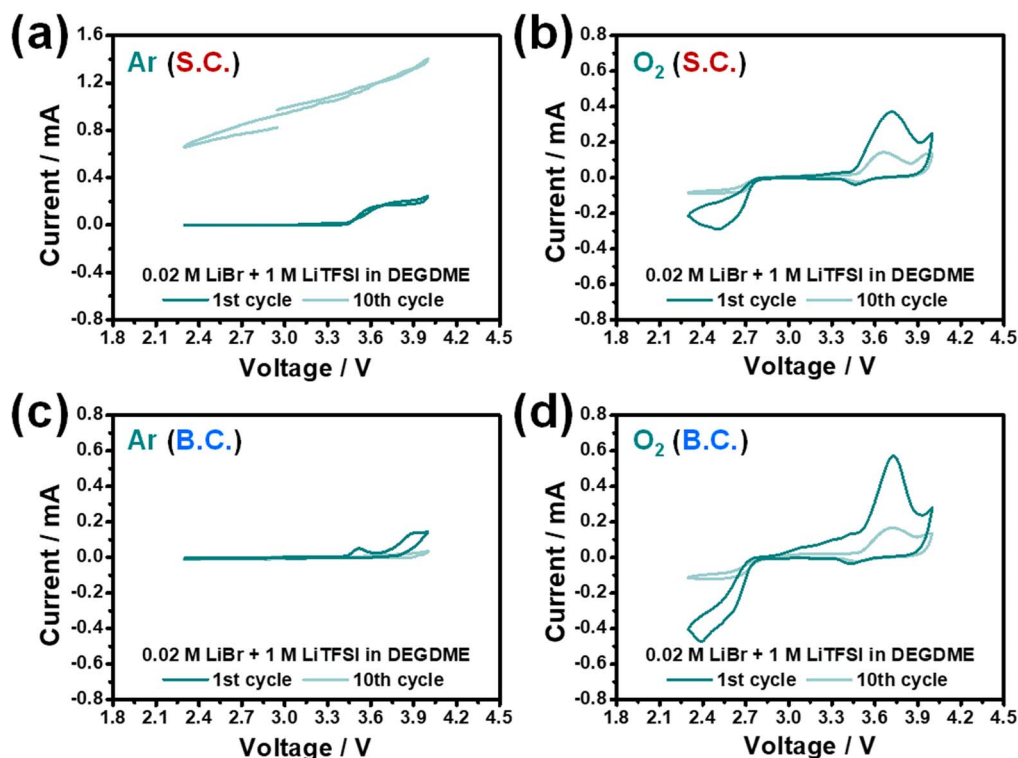


Figure 12. Comparative voltammetric charts of single (without SE) and bi-compartment cells (with SE), loaded with 1 M LiTFSI/DEGDME solutions containing 0.02 M LiBr under Ar and O₂ atmospheres as indicated, showing the first and 10th CV cycles; 0.05 mV s⁻¹, 2.3–4.0 V vs. Li. (a) and (b): single-compartment cells; (c) and (d): bi-compartment cells. (a) and (c): Ar atmosphere; (b) and (d): O₂ atmosphere. S.C. and B.C. indicate single or bi-compartment cells, respectively.

The halide RM has no possible intrinsic degradation mechanisms. Thus, the observed deactivation of cells is due to the well-known side reactions of the ether-based electrolyte solution with the reactive oxygen species formed during the ORR, which are accelerated by the presence of the halides as we already showed.⁵³ As was discussed in previous reports,^{38,53} reversible redox reactions of bromide and iodide may be promoted by the oxygen species with formation of materials such as the Li-O-Br and Li-O-I compounds.

Figure 14 further demonstrates the pronounced shuttle behavior of cells containing LiBr and LiI solutions under Ar atmosphere, at too low scanning rates. The response reflects the situation in which there is no limitation to crossover between the cathode and anode sides. This enables a pronounced reduction of the oxidized halides on the Li side, if the scanning rate is low enough, below the diffusion rates of Br₃⁻, Br₂, I₃⁻, and I₂. The increasing currents in the chart related to the LiBr solution reflect pronounced corrosion of the stainless-steel parts of the cells, owing to the presence of corrosive Br₃⁻ and Br₂ species, which is reflected by the high anodic currents. After being cycled with the solutions containing LiBr and LiI, cells were disassembled and their various parts were inspected and photographed, as presented in the images of Figure 14. The metallic parts related to the LiI solutions do not seem corroded, while the metallic parts related to the LiBr solutions are corroded. Hence, the reason for the increasing anodic currents in the cells containing LiBr under Ar is clear: pronounced corrosion of the stainless steel parts of the cells, owing to contact with the oxidized bromine species.

We already studied the behavior of single-compartment Li-O₂ cells containing LiI and LiBr as RMs.^{38,53} We discovered that the presence of LiI in these cells promotes the side reaction with water impurities in ether-based electrolyte solutions that irreversibly form LiOH deposits on the cathodes. In turn, such side reactions do not take place in the same ether-based electrolyte solutions containing LiBr during ORR.⁵³

Our previous work already discovered specific limitations in the use of LiI as an RM in Li-O₂ cells, which had not been ascertained by other researchers exploring these systems. Our previous work with solutions containing LiBr did not indicate such problems. However, in those studies, the experiments were relatively short. In the present work, long-term experiments were carried out, during which corrosion conditions could be developed.

Herein, we show severe problems with the use of LiBr in Li-O₂ cells caused by the unavoidable contact between the corrosive bromine species and metallic parts in the cells. Practically, it is impossible to fully avoid using metallic parts in these cells and fully isolate such parts from contact with the electrolyte solution. Therefore, it seems that the practical importance of LiBr as an RM in Li-O₂ cells is very limited.

The fact that all the RMs studied herein exhibit degradation in their electrochemical red-ox activity, even in bi-compartment cells under Ar atmosphere, is very surprising. Thus, it was important to find out whether the measured deactivation resulted from degeneration of the cells owing to destruction of the Li upon cycling and long-term operation.

Stability of redox mediators in narrow electrochemical voltage windows.—Figure 15 shows 10 voltammetric charts of experiments in which all the five RMs were tested in bi-compartment cells under Ar or O₂ atmospheres at slow scanning rates, within narrow potential domains varying between 300 to 450 mV depending on the RM used, as indicated. These narrow potential domains were adjusted to include only one reversible red-ox process, which is typically used in cycling tests of Li-O₂ batteries for each RM as indicated. All the cells demonstrated relatively stable behavior during 50 cycles (Figure 15), while the same cells and solutions operating within the wider potential domain (2.3–4.0 V) exhibited pronounced deactivation within the first few consecutive voltammetric cycles (Figures 6, 9, 10, 12, and 13).

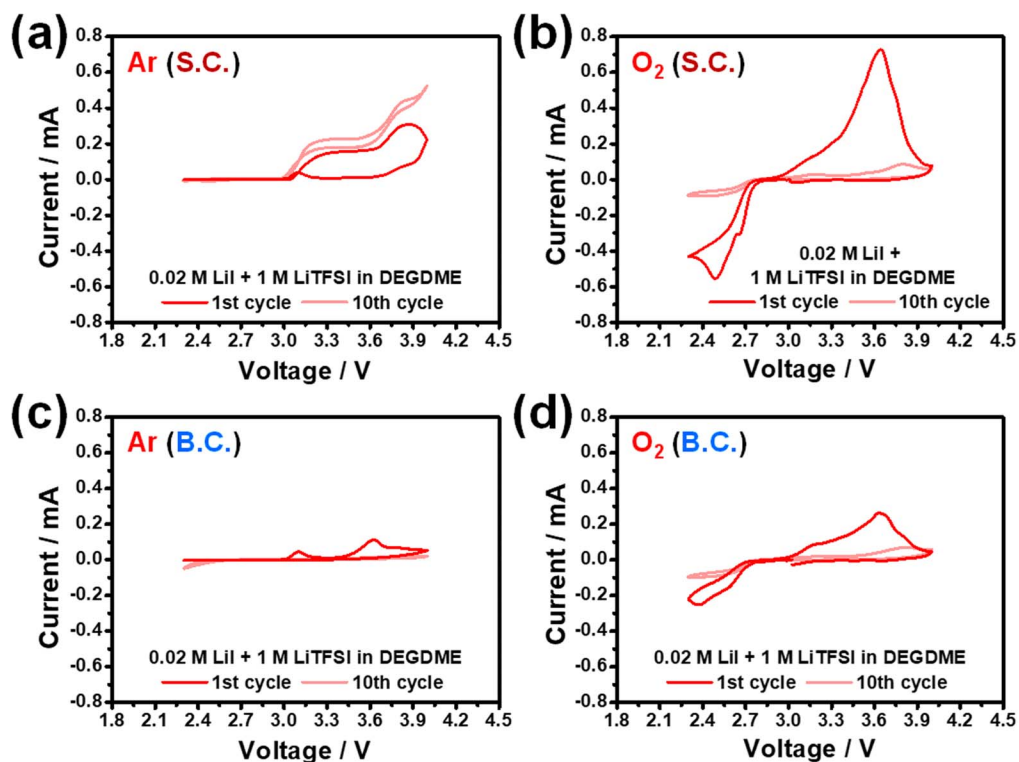


Figure 13. Comparative voltammetric charts of single (without SE) and bi-compartment cells (with SE), loaded with 1 M LiTFSI/DEGDME solutions containing 0.02 M LiI under Ar and O₂ atmospheres as indicated, showing the first and 10th CV cycles; 0.05 mV s⁻¹, 2.3–4.0 V vs. Li. (a) and (b): single-compartment cells; (c) and (d): bi-compartment cells. (a) and (c): Ar atmosphere; (b) and (d): O₂ atmosphere. S.C. and B.C. indicate single or bi-compartment cells, respectively.

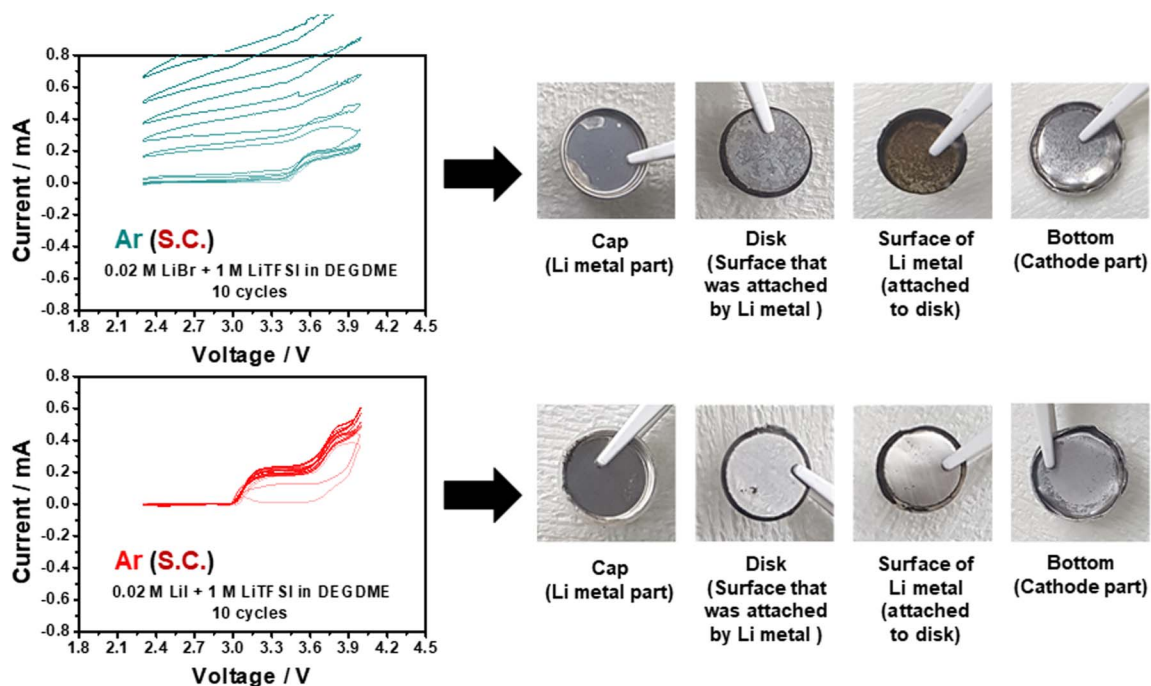


Figure 14. Photographs of single-compartment cell components after repeated voltammetric testing with 1 M LiTFSI/DEGDME solutions containing 0.02 M LiBr and LiI. The charts of the repeated CVs were performed with a scanning rate of 0.05 mV s⁻¹. Both CV charts reflect the shuttle mechanism: no cathodic reactions, owing to rapid chemical reduction of the bromine or iodine due to the Li anode. The cell containing LiBr reflects pronounced corrosion (high and increasing anodic currents). S.C. in the charts indicates single-compartment cells.

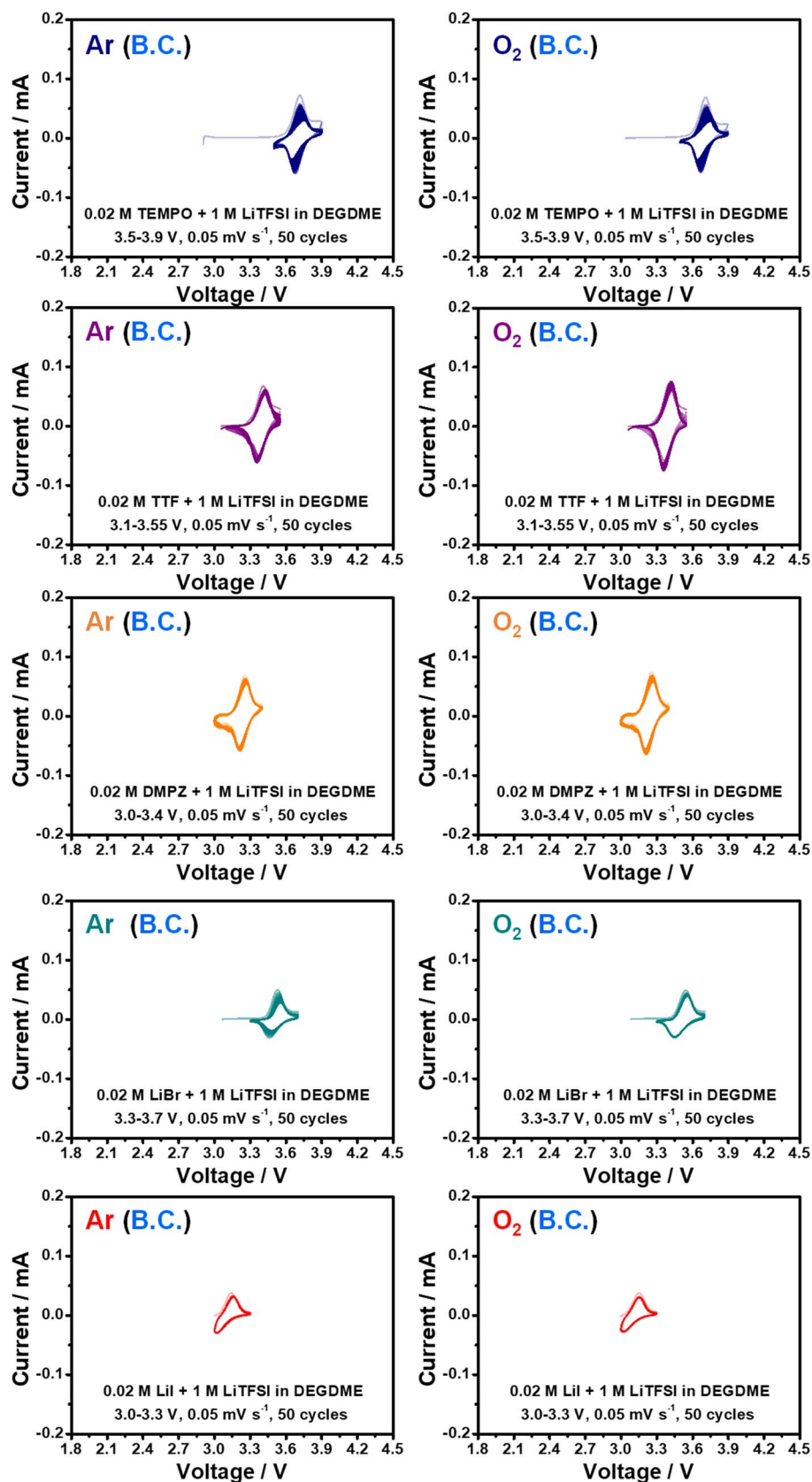


Figure 15. Comparative voltammetric charts of bi-compartment (B.C.) cells, loaded with 1 M LiTFSI/DEGDME solutions and 0.02 M redox-mediators under Ar or O₂ atmospheres, as indicated in the charts, showing progressive 50 consecutive cycling voltammograms at 0.05 mV s⁻¹. Cycling was performed at narrow voltage domains, as indicated.

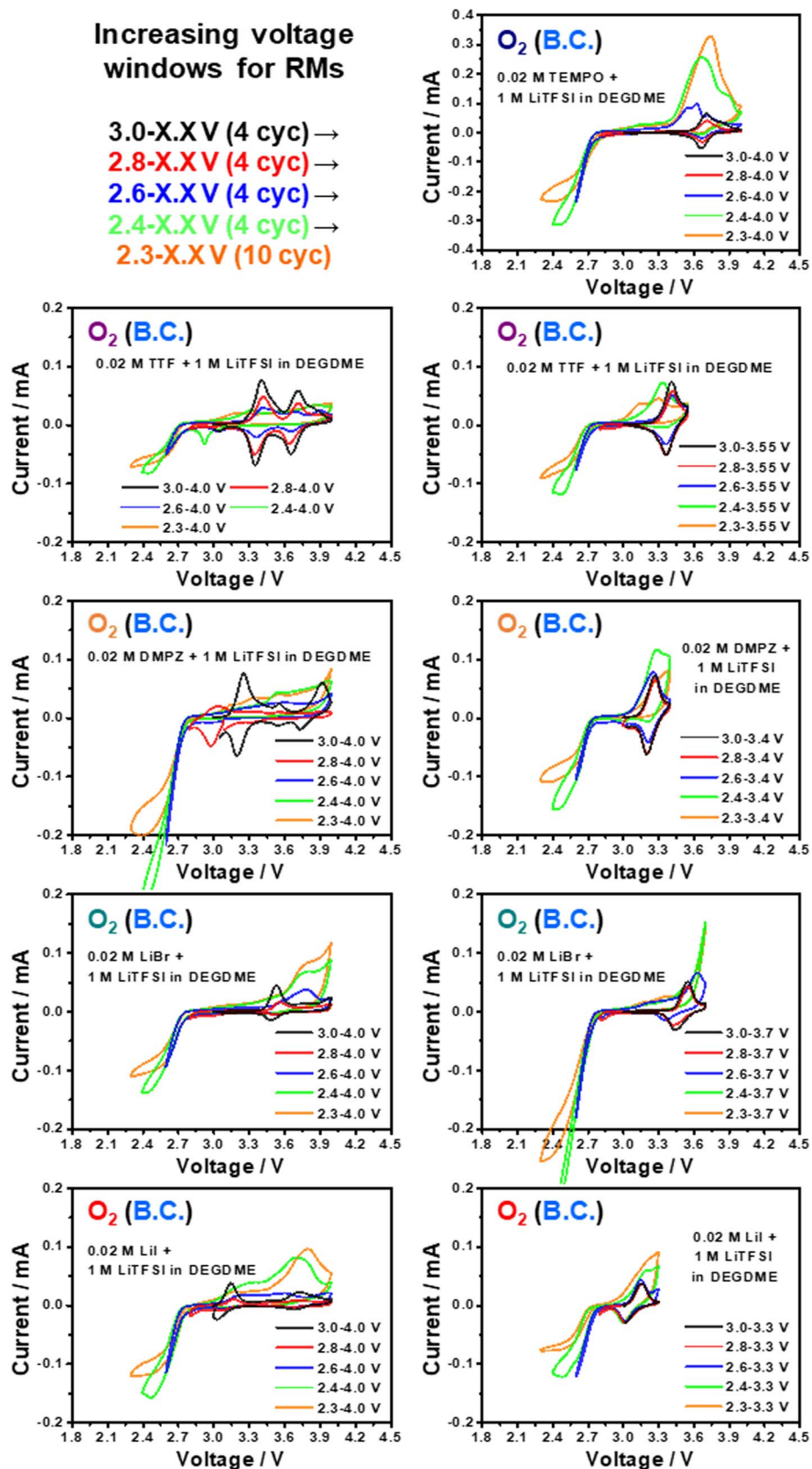


Figure 16. Comparative voltammetric charts of bi-compartment cells, loaded with 1 M LiTFSI/DEGDME solutions with 0.02 M redox-mediators under O₂ atmosphere cycled with a scan rate of 0.05 mV s⁻¹ in increasing potential ranges, as indicated. The upper potential limits were 4.0 V for TEMPO, 4.0 and 3.55 V for TTF, 4.0, and 3.4 V for DMPZ, 4.0 and 3.7 V for LiBr, and 4.0 and 3.3 V for LiI solutions (separate experiments). The lower potential limits were lowered after four cycles at each potential domain, as indicated. B.C. in the charts indicates bi-compartment cells.

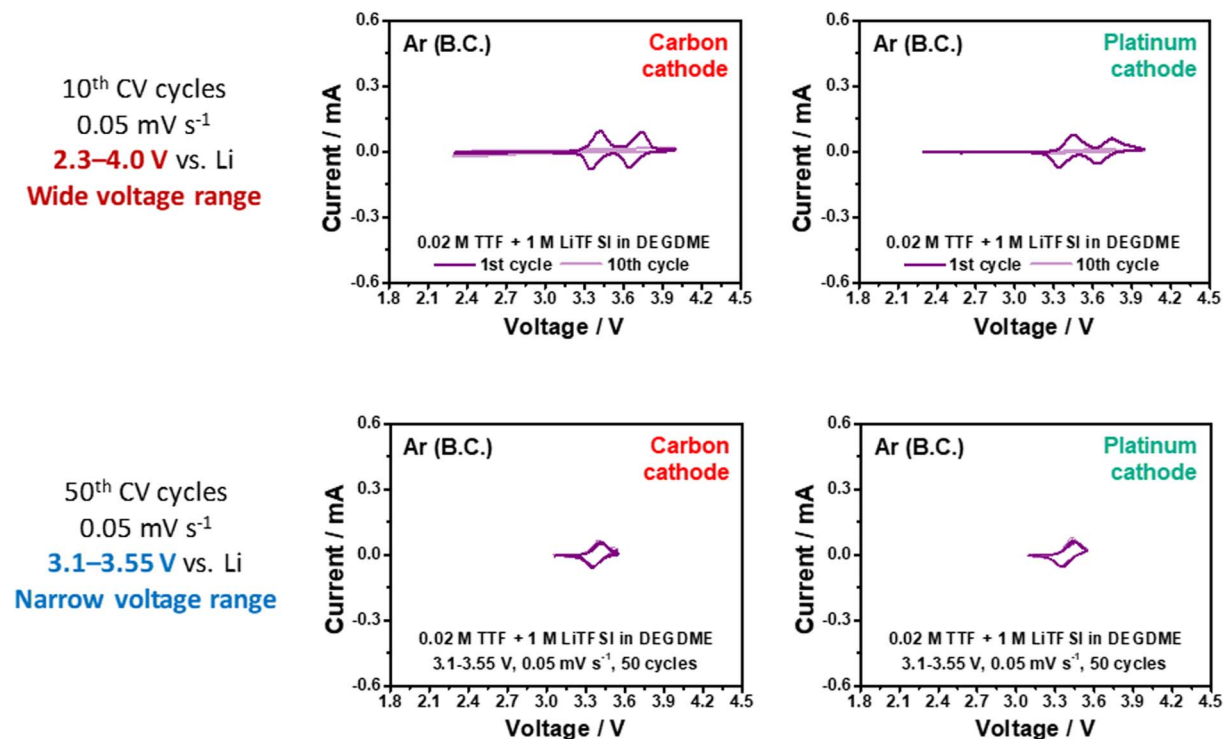


Figure 17. CV data using different electrodes (carbon and platinum) for checking the effect of cathode materials on deactivation of RMs.

Note that the accumulative charge in these experiments was similar to that in the experiments in which wide potential domains were applied. Figure 16 presents voltammetric charts of similar experiments (same cells and solutions), in which progressive voltammetric windows were applied as indicated. These experiments reveal that the Li metal side is not the reason for the observed deactivation of the electrochemical performance of the bi-compartments cells, because at narrow potential domains these two-compartments cells loaded with RMs solutions could undergo many dozens of cycles with no pronounced deactivation. Hence, the potential range of operation seems to play an important role, as indicated by the charts of Figures 15 and 16.

Moreover, controlled CV tests were conducted using Pt instead of carbon as an electrode to confirm the relationship between the type of cathode and decomposition of RM with wide and narrow voltage range, as shown in Figure 17. We confirmed that Pt electrodes in these cells exhibited the same tendency as the carbon electrodes: (1) deactivation of RMs at wide voltage range during cycling (Ar, Bi compartments cells) without O₂ and contact with Li metal anodes, (2) stable red-ox behavior of the RMs at narrow voltage ranges. Therefore, the cathode material itself (carbon or platinum), is not main issue for deactivation of the RMs studied herein.

It should be emphasized that a rigorous study on the behavior of each of the RMs chosen for this work and elucidation of the exact deactivation/degradation mechanisms was beyond the scope of this work. This comparative study was aimed at providing guidelines for selecting suitable RMs for Li-O₂ cells.

Conclusions

In this study, we focused on the suitability of selected, widely explored, RMs in Li-O₂ batteries under practical operation conditions. We have chosen for this study one of the most suitable and compatible solutions for these systems (LiTFSI/DEGDME). It should be noted that this solution is also unstable toward the superoxide and peroxide moieties formed in the solution phase by oxygen reduction, in the presence of Li cations. However, compared to other possible

non-aqueous electrolyte solutions, its use could provide a reasonable background for a study on the intrinsic limitations of the RMs that we explored. The present study on single and bi-compartments cells under Ar and O₂ atmospheres, using different RMs concentrations, rates, and voltage domains, enables to conclude that the organic RMs (TEMPO, TTF, and DMPZ) suffer from intrinsic instability when operating in the wide potential domains, relevant for non-aqueous Li-O₂ batteries (2.3–4.0 V). This instability owing to potential windows does not relate to the Li anode and/or oxygen reactions in these cells. The only mean that could be used for increasing the stability of the Li-O₂ cells containing these RMs was the control of the potential domains, by narrowing them. However, the narrow potential domains within which these RMs are stable, are not suitable for competed ORR and OER cycling. Regarding the use of LiI as a RM, its involvement in side reactions of ether-based electrolyte solution in Li-O₂ cells lowers its importance, despite previous reports on the promising use of LiI in Li-O₂ batteries (published before we discovered these aspects). LiBr, which was considered as an interesting RM in our previous work, was identified in the present study as a corrosive additive (in the form of Br₃⁻ and Br₂) during prolonged operation of Li-O₂ cells. Therefore, it seems that the present study should promote further search of more stable RMs for Li-O₂ batteries, as their role in these systems is critically important for reducing the detrimental over-potential of the charging process (oxygen evolution). Organometallic RMs, in which the red-ox active center (transition metal cation) is surrounded by cyclic organic ligands, may be found as more stable moieties in Li-O₂ cells in sufficiently wide potential windows. The study of such RMs in Li-O₂ batteries is the appropriate follow-up to the present study. We believe that this work provides a very good platform for an appropriate study of RMs and their useful evaluation with respect to Li-O₂ battery technology.

Acknowledgments

This work was supported by the research fund of Hanyang University (HY-2018) and was also supported by the Global Frontier R&D Program (2013M3A6B1078875) of the Center for Hybrid Interface

Materials (HIM) funded by the Ministry of Science, ICT & Future Planning.

ORCID

Won-Jin Kwak  <https://orcid.org/0000-0002-9807-1434>

Hun Kim  <https://orcid.org/0000-0002-3789-914X>

Hun-Gi Jung  <https://orcid.org/0000-0002-2162-2680>

Doron Aurbach  <https://orcid.org/0000-0002-1151-546X>

Yang-Kook Sun  <https://orcid.org/0000-0002-0117-0170>

References

- P. G. Bruce, S. A. Freunberger, L. J. Hardwick, and J. M. Tarascon, *Nat. Mater.*, **11**, 19 (2012).
- H.-G. Jung, J. Hassoun, J.-B. Park, Y.-K. Sun, and B. Scrosati, *Nat. Chem.*, **4**, 579 (2012).
- J. Lu, L. Li, J.-B. Park, Y.-K. Sun, F. Wu, and K. Amine, *Chem. Rev.*, **114**, 5611 (2014).
- X.-Y. Yang, J.-J. Xu, D. Bao, Z.-W. Chang, D.-P. Liu, Y. Zhang, and X.-B. Zhang, *Adv. Mater.*, **29**, 1700378 (2017).
- J. Kang, J. Kim, S. Lee, S. Wi, C. Kim, S. Hyun, S. Nam, Y. Park, and B. Park, *Adv. Energy Mater.*, **7**, 1700814 (2017).
- B. Zhou, L. Guo, Y. Zhang, J. Wang, L. Ma, W.-H. Zhang, Z. Fu, and Z. Peng, *Adv. Mater.*, **29**, 1701568 (2017).
- D. Sharon, P. Sharon, D. Hirshberg, M. Salama, M. Afri, L. J. W. Shimon, W.-J. Kwak, Y.-K. Sun, A. A. Frimer, and D. Aurbach, *J. Am. Chem. Soc.*, **139**, 11690 (2017).
- D. J. Lee, H. Lee, Y.-J. Kim, J.-K. Park, and H.-T. Kim, *Adv. Mater.*, **28**, 857 (2016).
- S. Ha, Y. Kim, D. Koo, K.-H. Ha, Y. Park, D.-M. Kim, S. Son, T. Yim, and K. T. Lee, *J. Mater. Chem. A*, **5**, 10609 (2017).
- D. Aurbach, B. D. McCloskey, L. F. Nazar, and P. G. Bruce, *Nat. Energy*, **1**, 16128 (2016).
- X. Yao, Q. Dong, Q. Cheng, and D. Wang, *Angew. Chem. Int. Ed.*, **55**, 11344 (2016).
- G. Girishkumar, B. McCloskey, A. C. Luntz, S. Swanson, and W. Wilcke, *J. Phys. Chem. Lett.*, **1**, 2193 (2010).
- B. D. McCloskey, R. Scheffler, A. Speidel, G. Girishkumar, and A. C. Luntz, *J. Phys. Chem. C*, **116**, 23897 (2012).
- V. Viswanathan, K. S. Thygesen, J. S. Hummelshøj, J. K. Nørskov, G. Girishkumar, B. D. McCloskey, and A. C. Luntz, *J. Chem. Phys.*, **135**, 214704 (2011).
- S. Meini, M. Piana, H. Beyer, J. Schwämmlein, and H. A. Gasteiger, *J. Electrochem. Soc.*, **159**, A2135 (2012).
- J.-L. Shui, J. S. Okasinski, P. Kenesei, H. A. Dobbs, D. Zhao, J. D. Almer, and D.-J. Liu, *Nat. Commun.*, **4**, 2255 (2013).
- I.-C. Jang, S. ida, and T. Ishihara, *ChemElectroChem*, **2**, 1380 (2015).
- M. H. Cho, J. Trottier, C. Gagnon, P. Hovington, D. Clément, A. Vijh, C.-S. Kim, A. Guerfi, R. Black, L. Nazar, and K. Zaghi, *J. Power Sources*, **268**, 565 (2014).
- A. C. Luntz and B. D. McCloskey, *Chem. Rev.*, **114**, 11721 (2014).
- M. M. O. Thotiyil, S. A. Freunberger, Z. Peng, and P. G. Bruce, *J. Am. Chem. Soc.*, **135**, 494 (2013).
- B. D. McCloskey, A. Speidel, R. Scheffler, D. C. Miller, V. Viswanathan, J. S. Hummelshøj, J. K. Nørskov, and A. C. Luntz, *J. Phys. Chem. Lett.*, **3**, 997 (2012).
- A. Debart, A. J. Paterson, J. Bao, and P. G. Bruce, *Angew. Chem.*, **120**, 4597 (2008).
- Y. C. Lu, Z. Xu, H. A. Gasteiger, S. Chen, K. H. Schifferli, and Y. Shao-Horn, *J. Am. Chem. Soc.*, **132**, 12170 (2010).
- H.-G. Jung, Y. S. Jeong, J.-B. Park, Y.-K. Sun, B. Scrosati, and Y. J. Lee, *ACS Nano*, **7**, 3532 (2013).
- E. Yilmaz, C. Yogi, K. Yamanaka, T. Ohta, and H. R. Byon, *Nano Lett.*, **13**, 4679 (2013).
- B. G. Kim, H. J. Kim, S. Back, K. W. Nam, Y. Jung, Y. K. Han, and J. W. Choi, *Sci. Rep.*, **4**, 4225 (2014).
- W.-J. Kwak, K. C. Lau, C. D. Shin, K. Amine, L. A. Curtiss, and Y.-K. Sun, *ACS Nano*, **9**, 4129 (2015).
- W.-J. Kwak, T.-G. Kang, Y.-K. Sun, and Y. Lee, *J. Mater. Chem. A*, **4**, 7020 (2016).
- B. D. McCloskey and D. Addison, *ACS Catal.*, **7**, 772 (2017).
- J.-B. Park, S. H. Lee, H.-G. Jung, D. Aurbach, and Y.-K. Sun, *Adv. Mater.*, **30**, 1704162 (2018).
- B. D. McCloskey, R. Scheffler, A. Speidel, D. S. Bethune, R. M. Shelby, and A. C. Luntz, *J. Am. Chem. Soc.*, **133**, 18038 (2011).
- B. D. McCloskey, A. Valery, A. C. Luntz, S. R. Gowda, G. M. Wallraff, J. M. Garcia, T. Mori, and L. E. Krupp, *J. Phys. Chem. Lett.*, **4**, 2989 (2013).
- K. Sakaushi, T. P. Fellingner, and M. Antonietti, *ChemSusChem*, **8**, 1156 (2015).
- Y. Chen, S. A. Freunberger, Z. Peng, O. Fontaine, and P. G. Bruce, *Nat. Chem.*, **5**, 489 (2013).
- B. J. Bergner, A. Schurmann, K. Peppler, A. Garsuch, and J. Janek, *J. Am. Chem. Soc.*, **136**, 15054 (2014).
- H.-D. Lim, B. Lee, Y. Zheng, J. Hong, J. Kim, H. Gwon, Y. Ko, M. Lee, K. Cho, and K. Kang, *Nat. Energy*, **1**, 16066 (2016).
- T. Liu, M. Leskes, W. Yu, A. J. Moore, L. Zhou, P. M. Bayley, G. Kim, and C. P. Grey, *Science*, **350**, 530 (2015).
- W.-J. Kwak, D. Hirshberg, D. Sharon, M. Afri, A. A. Frimer, H.-G. Jung, D. Aurbach, and Y.-K. Sun, *Energy Environ. Sci.*, **9**, 2334 (2016).
- D. Sun, Y. Shen, W. Zhang, L. Yu, Z. Yi, W. Yin, D. Wang, Y. Huang, J. Wang, D. Wang, and J. B. Goodenough, *J. Am. Chem. Soc.*, **136**, 8941 (2014).
- D. Kundu, R. Black, B. Adams, and L. F. Nazar, *ACS Cent. Sci.*, **1**, 510 (2015).
- N. Feng, P. He, and H. Zhou, *ChemSusChem*, **8**, 600 (2015).
- B. J. Bergner, M. R. Busche, R. Pinedo, B. B. Berkes, D. Schroder, and J. Janek, *ACS Appl. Mater. Interfaces*, **8**, 7756 (2016).
- T. Zhang, K. Liao, P. He, and H. Zhou, *Energy Environ. Sci.*, **9**, 1024 (2016).
- B. G. Kim, J.-S. Kim, J. Min, Y.-H. Lee, J. H. Choi, M. C. Jang, S. A. Freunberger, and J. W. Choi, *Adv. Funct. Mater.*, **26**, 1747 (2016).
- W. R. Torres, S. E. Herrera, A. Y. Tesio, M. d. Pozo, and E. J. Calvo, *Electrochimica Acta*, **182**, 1118 (2015).
- S. H. Lee, J.-B. Park, H.-S. Lim, and Y.-K. Sun, *Adv. Energy Mater.*, **7**, 1602417 (2017).
- W.-J. Kwak, H.-G. Jung, D. Aurbach, and Y.-K. Sun, *Adv. Energy Mater.*, **7**, 1701232 (2017).
- B. G. Kim, C. Jo, J. Shin, Y. Mun, J. Lee, and J. W. Choi, *ACS Nano*, **11**, 1736 (2017).
- Z. Guo, C. Li, J. Liu, Y. Wang, and Y. Xia, *Angew. Chem. Int. Ed.*, **56**, 7505 (2017).
- Y. Li, S. Dong, B. Chen, C. Lu, K. Liu, Z. Zhang, H. Du, X. Wang, X. Chen, X. Zhou, and G. Cui, *J. Phys. Chem. Lett.*, **8**, 4218 (2017).
- X. Xin, K. Ito, and Y. Kubo, *ACS Appl. Mater. Interfaces*, **9**, 25976 (2017).
- W.-J. Kwak, S.-J. Park, H.-G. Jung, and Y.-K. Sun, *Adv. Energy Mater.*, **8**, 1702258 (2018).
- W.-J. Kwak, D. Hirshberg, D. Sharon, H.-J. Shin, M. Afri, J.-B. Park, A. Garsuch, F. F. Chesneau, A. A. Frimer, D. Aurbach, and Y.-K. Sun, *J. Mater. Chem. A*, **3**, 8855 (2015).
- C. M. Burke, R. Black, I. R. Kochetkov, V. Giordani, D. Addison, L. F. Nazar, and B. D. McCloskey, *ACS Energy Lett.*, **1**, 747 (2016).
- Y. G. Zhu, Q. Liu, Y. Rong, H. Chen, J. Yang, C. Jia, L.-J. Yu, A. Karton, Y. Ren, X. Xu, S. Adams, and Q. Wang, *Nat. Commun.*, **8**, 14308 (2017).
- M. Tulodziecki, G. M. Leverick, C. V. Amanchukwu, Y. Katayama, D. G. Kwabi, F. Barde, P. T. Hammond, and Y. Shao-Horn, *Energy Environ. Sci.*, **10**, 1828 (2017).
- Y. Qiao, S. Wu, Y. Sun, S. Guo, J. Yi, P. He, and H. Zhou, *ACS Energy Lett.*, **2**, 1869 (2017).
- H. Yang, Q. Wang, R. Zhang, B. D. Trimm, and M. S. Whittingham, *Chem. Commun.*, **52**, 7580 (2016).
- W.-J. Kwak, S. H. Ha, D. H. Kim, K. H. Shin, Y.-K. Sun, and Y. J. Lee, *ACS Catal.*, **7**, 8192 (2017).
- B. J. Bergner, C. Hofmann, A. Schurmann, D. Schroder, K. Peppler, P. R. Schreiner, and J. Janek, *Phys. Chem. Chem. Phys.*, **17**, 31769 (2015).
- Y. Hase, J. Seki, T. Shiga, F. Mizuno, H. Nishikoori, H. Iba, and K. Takechi, *Chem. Commun.*, **52**, 12151 (2016).
- X. Gao, Y. Chen, R. Johnson, Z. P. Jovanov, and P. G. Bruce, *Nat. Energy*, **2**, 17118 (2017).
- Y. Qiao and S. Ye, *J. Phys. Chem. C*, **120**, 15830 (2016).
- C. Yang, J. Han, P. Liu, C. Hou, G. Huang, T. Fujita, A. Hirarta, and M. Chen, *Adv. Mater.*, **29**, 1702752 (2017).
- J. Han, G. Huang, Y. Ito, X. Guo, T. Fujita, P. Liu, A. Hirarta, and M. Chen, *Adv. Energy Mater.*, **7**, 1601933 (2017).
- Z. Liang and Y.-C. Lu, *J. Am. Chem. Soc.*, **138**, 7574 (2016).
- S. H. Lee, W.-J. Kwak, and Y.-K. Sun, *J. Mater. Chem. A*, **5**, 15512 (2017).
- D. S. Kim and Y. J. Park, *J. Alloys Compd.*, **591**, 164 (2014).
- T. H. Yoon and Y. J. Park, *RSC Adv.*, **4**, 17434 (2014).
- H.-D. Lim, H. Song, J. Kim, H. Gwon, Y. Bae, K.-Y. Park, J. Hong, H. Kim, T. Kim, Y. H. Kim, X. Lepro, R. Ovalle-Robles, R. H. Baughman, and K. Kang, *Angew. Chem. Int. Ed.*, **53**, 3926 (2014).
- M. Yu, X. Ren, L. Ma, and Y. Wu, *Nat. Commun.*, **5**, 5111 (2014).
- Y. G. Zhu, C. Jia, J. Yang, F. Pan, Q. Huang, and Q. Wang, *Chem. Commun.*, **51**, 9451 (2015).
- J. Yi, S. Wu, S. Bai, Y. Liu, N. Li, and H. Zhou, *J. Mater. Chem. A*, **4**, 2403 (2016).
- X. Zeng, L. Leng, F. Liu, G. Wang, Y. Dong, L. Du, L. Liu, and S. Liao, *Electrochim. Acta*, **200**, 231 (2016).
- W. Zhang, Y. Shen, D. Sun, Z. Huang, J. Zhou, H. Yan, and Y. Huang, *Nano Energy*, **30**, 43 (2016).
- C. K. Lee and Y. J. Park, *ACS Appl. Mater. Interfaces*, **8**, 8561 (2016).
- H. Beyer, S. Meini, N. Tsiouvaras, M. Piana, and H. A. Gasteiger, *Phys. Chem. Chem. Phys.*, **15**, 11025 (2013).
- X. Yao, Q. Dong, Q. Cheng, and D. Wang, *Angew. Chem. Int. Ed.*, **55**, 11344 (2016).
- V. K. C. Chau, Z. Chen, H. Hu, and K.-Y. Chan, *J. Electrochem. Soc.*, **164**, A284 (2017).
- R. F. Nelson, D. W. Leedy, E. T. Seo, and R. N. Adams, *Z. Anal. Chem.*, **224**, 184 (1966).
- H.-D. Lim, B. Lee, Y. Bae, H. Park, Y. Ko, H. Kim, J. Kim, and K. Kang, *Chem. Soc. Rev.*, **46**, 2873 (2017).
- D. Sharon, V. Etacheri, A. Garsuch, M. Afri, A. A. Frimer, and D. Aurbach, *J. Phys. Chem. Lett.*, **4**, 127 (2013).
- Z. Liang, Q. Zou, Y. Wang, and Y.-C. Lu, *Small Methods*, **1**, 1700150 (2017).
- Y. Qiao and S. Ye, *J. Phys. Chem. C*, **120**, 8033 (2016).